*Author:*
**Ji, Hexuan**

*Title:*
**An automated system for disassembly of mobile phones at their end of life**

# An automated system for

# disassembly of mobile phones at their end of life

By Hexuan Ji

September 2022

A dissertation submitted to the University of Bristol in accordance with the requirements for award of the degree of Master of Science by research in the Faculty of Engineering

Word count: 10927

# Abstract

In the context of the current increase in demand for E-waste recycling, this thesis proposes a solution for the recycling of used cell phones to dismantle used cell phones with the necessary mechanical motion provided through a Stewart Platform. A digital model of the platform is constructed encompassing the kinematics and dynamics properties of the system to assess the feasibility of the solution providing the required trajectory of the end effector to complete the translational and rotational motions necessary for disassembly. A series of experiments were conducted to measure the maximum force required to disassemble mobile phone screens, which in most cases is the largest force in the disassembly process to inform the design of the disassembly platform. The resulting analyses showing the effectiveness of the method are provided followed by suggested future work to create a complete disassembly system based on the investigated framework.

# Dedication and Acknowledgements

The process of completing this thesis was extremely difficult, but I am very thankful that I was able to receive a lot of academic help from my supervisor Professor Aydin despite the influence of COVID-19. At the same time, I would like to thank Dr Maria for her guidance and advice in the process of writing this thesis. Thanks to all the people who helped me during the experiment. I appreciate my parents for their moral encouragement and support.

# Author’s Declaration

I declare that the work in this dissertation was carried out in accordance with the requirements of the University's Regulations and Code of Practice for Research Degree Programmes and that it has not been submitted for any other academic award. Except where indicated by specific reference in the text, the work is the candidate's own work. Work done in collaboration with, or with the assistance of, others, is indicated as such. Any views expressed in the dissertation are those of the author.

SIGNED: Hexuan Ji DATE: 20 September 2022

# Table of Contents

# Figure contents

# 1.Introduction

## 1.1 The background

Nowadays, with the progress of technology and the development of human society, there is more and more E-waste. As per the recent reports by the United Nations (UN), in 2021, on an average, each person is expected to generate about 7.6 kg per capita of E-waste, resulting in a massive amount of 57.4 MMT（Metal Metric Ton） across the globe (Murthy and Ramakrishna 2022). E-waste is particularly evident, and there is no good and well-established recycling system for electronic equipment. This is believed to be due to a number of reasons, including the development of networking and internet use, technological advances and rapid change, rising living standards and lack of consumer awareness (Foo, Kara, and Pagnucco 2022a).

Waste mobile phones, as a type of small-size E-waste, has been one of the largest and fastest-growing waste streams in the world (Liu et al. 2022). For example, the service life of a smartphone is limited and cannot be used permanently, and core components such as batteries will gradually age with use. And cell phone manufacturers in order to update the iteration of the product to obtain more profits, will continue to launch new products to attract consumers to buy. And the battery and other core components are also integrated in the phone, and not removable. That's why modern people update their smartphones very frequently.

As sales grow, the precious metals and materials needed to produce smartphones become even more scarce. Mobile devices contain conflict elements like gold, toxic ones like arsenic and rare elements like indium. For the European Union it is reported that 74,900 tons of lithium-ion batteries are placed on the EU market in 2019, of which 49% are related to electrical and electronic equipment applications, and 51% are industrial and auto-motive batteries (Windisch-Kern et al. 2022). As lithium cathodes degrade over time, these cells cannot be used in fresh batteries. Lithium battery dumps can burn for years, releasing harmful chemicals into the atmosphere that affect the way we breathe and contribute to global warming batteries (Windisch-Kern et al. 2022).

These facts show that how to deal with old and waste smart phones as the representative of the electronic waste is an urgent problem in the world, which is not only related to the environmental

pollution from the surface, but also related to the deeper economic problems. If the recycling of used cell phones can be carried out effectively, it can not only alleviate the problem of environmental pollution to a certain extent, but also create some economic value from two aspects: the first aspect is that because the traditional way of using land for landfill will take up land and cannot create greater economic benefits; the second aspect is that if there is a suitable and efficient way to recycle used mobile phone parts that can still be used, each cell phone manufacturer's parts suppliers can control the cost and do not have to start manufacturing parts from the first step, which is a good thing for cell phone manufacturers to save money. Further, from the consumer's point of view, if cell phone manufacturers and their component suppliers can better control costs, it is obvious that the price of products will be better controlled, and consumers can spend less money to buy new smart phones.

In summary, it is valuable to study how to find a green and efficient way to dispose of used cell phones.

## 1.2 The existing ways to deal with waste mobile phones

E-waste disposal is now a major problem due to the high economic outlay required for fine sorting and recycling of E-waste, limited landfill space, incineration treatment, unsuitable recycling, high contaminants (metals, metalloids and volatile organic compounds) and mostly informal E-waste recycling (Sanito, You, and Wang 2021).

Some of the traditional ways of dealing with E-waste have major drawbacks. For example: the landfill method requires a large area of land, and need to dig a very deep pit to fill a large amount of electronic waste, first of all, digging a large pit requires a lot of human and material resources and there are some safety hazards, secondly, this part of the land due to heavy metals in electronic waste will lead to this land for landfill, including the surrounding land cannot be cultivated, and often use large machinery for landfill work, will The frequent use of large machinery for landfill work will make a large area around the non-residential area, and cannot develop real estate; The use of incineration can cause similar problems, generating large amounts of toxic and harmful gases, and is a great waste of resources. These are the disadvantages of the landfill and incineration

methods. But it is undeniable that these traditional ways of dealing with E-waste have some advantages in the short term, such as simple processes, low cost of operation, no assembly line operations to pick parts, saving labor costs, etc. Therefore, if people can find a way to deal with used cell phones in a way that takes into account the economic cost and the final recycling effect, it is the best solution to solve the problem of recycling used cell phones, which means that the solution can take into account the green issues and also be able to identify and recover the valuable parts of used cell phones in an efficient way without requiring too much labor cost.

The complex structure of used cell phones and the wide variety of different models of cell phones have brought great difficulties to the recycling of used cell phones. Considering these factors, the whole process of recycling parts from used cell phones can be divided into the following stages: first dismantling the used cell phones, then identifying and judging which parts are worth recycling (reusable), and then sorting and recycling these parts.

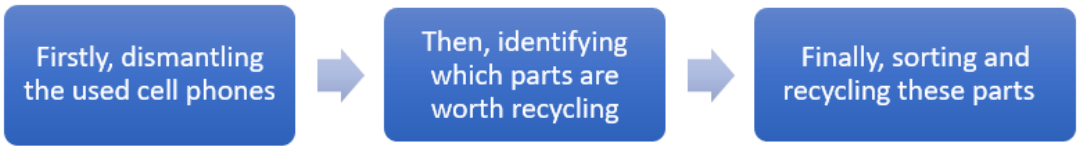


*Figure 1.1- Process of recycling wasted phones*

So how to efficiently dismantle used cell phones is one of the most important steps in the whole recycling process.

Research on non-destructive dismantling of cell phones is still in its infancy (H. Li et al. 2022). And the method of destructive disassembly of cell phones is generally manual disassembly, which is still used in most countries. There are already processing solutions to solve this problem by manually identifying the type of phone through an identification system and placing the used phone on a frame, after which the phone is disassembled automatically in six stations (Kopacek and Kopacek 2003). This method is indeed efficient and practical, but there are still some drawbacks. Since this method is mainly for non-smart phones, the assembly method of smart phones is more complicated than that of older phones, and the milling process in this method can cause damage to some parts that could have been recycled due to high local temperatures.

For smartphones, the use of computer vision technology to identify the phone model, followed by clamping, heating and disassembly is a very sophisticated and effective (Ambrosch et al. 2018). However, the disadvantage of this method is that it can only be disassembled for specific models of cell phones, and for some phones with complex assembly methods, the process of removing the back cover or screen and unscrewing the screws requires manual operation. This reduces the efficiency of the whole process, and the complexity of the manual operation and the level of detail required makes the application scenario of this system limited.

In order to efficiently and non-destructively dismantle cell phones, Apple has launched three robots: "Liam", "Daisy" and "Dave." Although it is now possible to completely disassemble a phone within 20 seconds, the problem is that Apple's disassembly robot is only able to disassemble various models of iPhones, and can do nothing for other brands of phones (H. Li et al. 2022). The above examples show the following issues. First of all, from the technical level, there are technical means to complete the dismantling of a cell phone in a non-destructive way in a relatively short time (20 seconds); the main challenge of the current non-destructive fully automated dismantling of cell phones is how to automatically identify the model of the phone and be able to effectively dismantle all or most of the phones and recycle the parts; dismantling different brands and models of cell phones. The workflow required to disassemble different brands and models of cell phones differs, which also indicates the difference in the internal structure or assembly method of these phones.

## 1.3 A new solution

Apple's "Liam" robot, for example, was designed for the disassembly of a batch of iPhone 6. Since the company itself knows all the design parameters and only disassembles this one model of phone, the position of the working parts is fixed at a fixed station (Rujanavech et al. 2016). And there is no need to identify and position the parts, because the design dimensions of the parts of the same batch of phones are fixed. The efficiency of this robot is based on the premise that the phones are of the same model and the design dimensions are known, which is not universal. Moreover, although robots like this are efficient and stable, they are extremely inflexible, and the cost of

conversion is extremely high; if you want to disassemble other models of cell phones of other brands, you almost need to redesign the whole assembly line. This is not in line with the original intent of the problem.

A reasonable solution for non-destructive dismantling of used cell phones should meet the following requirements: fully automated, universal (can automatically identify and dismantle most cell phones), stable and efficient.

In applications requiring high load capacity and precise positioning, parallel manipulators are a better choice (Patel and George 2012). Parallel manipulators are widely used in industry over decades because of their excellent dynamic agility, high load-to-weight ratio, distributed joint errors, and simple inverse kinematics (Yang, Ye, and Li 2022). In many cases where stability and high motion accuracy are required, parallel manipulators can be used.

The parallel manipulators use several related serial chains to connect the upper platform. The error of each chain is independent but being average not accumulated on the platform, which means better precision and stability.

The Stewart Platform is a kind of parallel manipulators, commonly used as motion bases. It uses pairs of universal ball joints to connect the legs between the base and the top plate. Using prismatic actuators on each leg to motivate the device, possessing six degrees of freedom. Using the Stewart Platform to carry the waste phones can meet the requirements of sufficient stability, high degree of freedom. This study takes Stewart Platform as an example and thus proposes a solution as shown below.

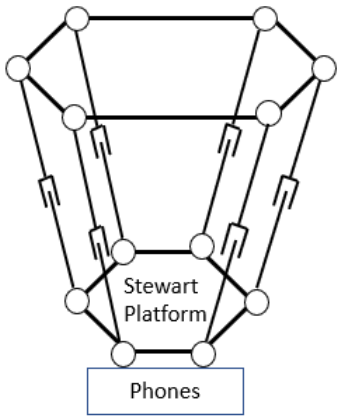


*Figure 1.1 - Stewart Platform configuration*

The used phone is fixed on a flat surface and above it is the inverted Stewart Platform fixed by the base. Using computer vision to recognize the components and locate them. The screen is disassembled by the movement of the end effector in the vertical direction and the parts are moved by the movement on the flat surface. The screws are removed by rotating around the $Z$ axis. The specific issues involved in the process are further explained later in the next chapters.

# 2 Research Framework

## 2.1 Research objective

Based on the following characteristics of the used cell phone recycling problem mentioned in the previous section, the problem to be solved is first analyzed and characterized. The number of used cell phones is huge; used cell phones contain valuable components and metal elements; traditional recycling methods for used cell phones cause great pollution to the environment; and the existing automatic recycling methods for used cell phones are not very popular. And this study initially proposes a scheme to complete the disassembly of used cell phones by using the Stewart platform in the previous paper. With this scheme, the disassembly of cell phone screen and the removal of internal screws can be satisfied. What's more, this method does not need to add extra motors for the electric screwdriver, so this method has some economic benefits.

Therefore, the purpose of this study is to build a model and perform simulations to validate the feasibility of the model based on the research conducted on the Stewart platform. The process of removing the screen is selected and experiments are conducted to measure the maximum force required to remove the screen from the phone. The experimental results are analyzed and the maximum force required for the actuators on each piston of the Stewart platform during the screen removal process is calculated.

According to the objective of the study, the solution should first be analyzed in terms of the problems involved and a thorough literature survey should be conducted to demonstrate the significance of the study and to investigate whether the relevant technology supports the solution. A simplified version of the model is completed by adding materials based on the prevailing material of each part and adding individual joints to impose constraints. The kinematic model is then built

based on the kinetic principles, and the simplified version of the model completed in the previous step is replaced in the kinematic simulation to verify the correctness of the kinematic model. After that, the actual measurement of the force required to disassemble the phone is needed, and the experiment focuses on the process of disassembling the phone screen. The purpose of the experiment is to actually measure the tensile force required to disassemble the mobile phone screen and to conduct further experiments to measure the maximum force required to disassemble the sample during the process of disassembling the cell phone screen. After completing the experiment, the data is processed to find and calculate the maximum force required to disassemble the screen with a high degree of confidence that can be applied to most cell phones of the same model as the sample. The model is then used to calculate how much force is needed to operate the actuator of the prismatic joint of the Stewart platform, thus demonstrating the feasibility of the solution proposed in this thesis.

Therefore, this thesis will be developed in the following manner.

1. In the literature review section, review existing techniques for recycling cell phones, new techniques for recycling cell phones, methods for locating parts on cell phones using computer vision techniques, and research progress on automated disassembly of cell phones.
2. In the theoretical framework section, the theoretical basis applied to the modeling of the Stewart Platform will be presented.
3. In the experimental section, the process of the experiment is shown.
4. In the results section, the simulation is used to verify whether the model can be controlled to move according to the target trajectory. The results of the experimental part will be analyzed.
5. The maximum force of each actuator is calculated.

# 3 Literature review

The previous sections shows that recycling used smartphones is economically and environmentally beneficial, but there is no mature and efficient technology that is universally applicable to all brands and models of used phones. One of the reasons that hinder the development of this technology is that the parameters of disassembly vary from phone to phone and are difficult to measure. Therefore, the main objective of this study is to propose a feasible disassembly solution for used phones and to design a measurement method to measure the maximum force required for the disassembly process of the same model of used phone and to design a platform to carry this model of used phone accordingly.

Considering this objective, the literature review chapter has the following goals.

1. To clarify the various components required for a recycling used and end-of-life cell phone project and to identify areas of research to be considered in developing a solution
2. To investigate the various methods that can be used to recycle used cell phones and to compare them
3. Examples of using computer vision to identify and locate parts
4. Applications of The Stewart Platform
5. Current solutions in engineering

The results of the literature review are used to inform the research questions and objectives that will guide the rest of the paper. The literature review is structured as follows.

It is first necessary to have an overall understanding of the problem under study, which includes the background and the various areas involved, so that the subsequent research studies are focused on the subject. After that it is necessary to review the various methods of recycling used cell phones, especially those related to the field of engineering. After completing the review of these methods a deeper understanding of the advantages and limitations of each method can be obtained and in the process the purpose of this study can be emphasized.

Secondly, what difficulties exist in the process of recycling cell phones and in each segment of the engineering field. What techniques are available in each segment to solve similar problems. This section can be more helpful to understand the overall research objectives and will give a more

detailed understanding of each part.

Finally, the first two parts allow the identification of the problem that needs to be solved if a new solution is to be proposed, and further investigation of the technologies related to this problem. The feasibility of the relevant technologies is understood by investigating the application of these technologies to solve similar problems. After that, the focus of the research can be on the specific problem.

## 3.1 General introduction

The background of the study has been explained in the 'Introduction' chapter, and it can be seen that there is a large amount of E-waste and a large number of used cell phones. There are many parts of used cell phones that are still valuable for recycling, but traditional recycling methods cause pollution problems, and there is no well-established automated green recycling method that works for most models of used cell phones, so it makes economic sense to design an automated way of recycling valuable parts of used cell phones that meets the needs.

The global generation of waste electrical and electronic equipment is expected to exceed 75 million tons by 2030 (Shittu, Williams, and Shaw 2021). As a representative of electronic waste, the large and growing number of used cell phones, which cannot be properly disposed of, has a serious negative impact on the environment (Lisińska, Saternus, and Willner 2018). Used cell phones contain toxic elements such as lead, mercury, chromium, nickel, beryllium, antimony and arsenic, as well as valuable metals such as gold, silver, palladium and platinum (Osibanjo and Nnorom 2008) . The distribution of metal elements in each part of the PCB board on both sides is shown in Figure 3.1 (Lee, Kim, and Lee 2012) .So it has some economic benefits if effective methods can be used to recycle the metal parts that can be reused in used cell phones.

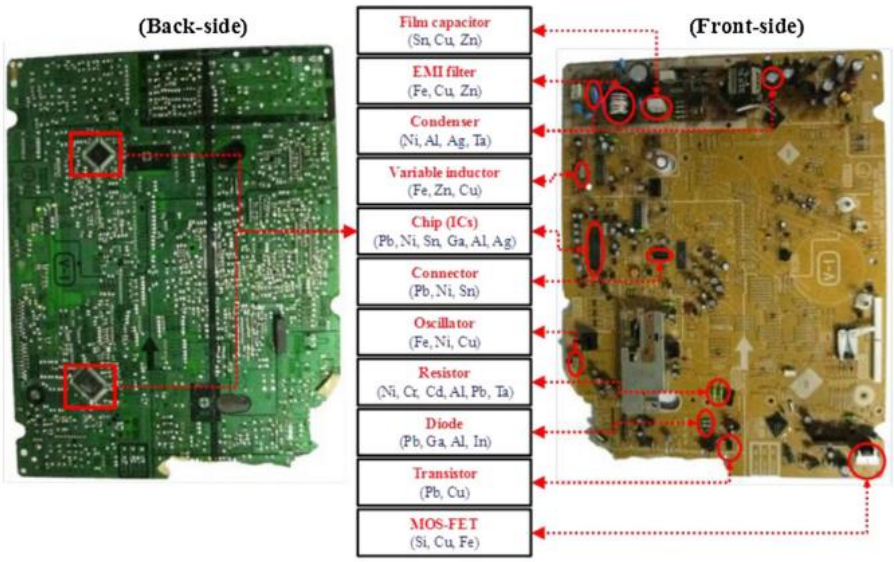


*Figure 3.1-Distribution of metal elements in each part of the PCB board (Lee, Kim, and Lee 2012)*

Not only the metal elements, but also the structural parts such as screws contained in used cell phones have the value of recycling at the same time, the structure of used cell phones is complex, and the quantity is huge if the disposal is done in bulk. This brings great difficulties to the recycling of used cell phones. Therefore, how to effectively deal with different types of used cell phones is the focus of research. As a result, many researchers have studied topics related to the disassembling of used cell phones.

An effective and less hazardous system, an ammonia solution of copper sulfate, is used to leach elemental gold from printed circuit boards (PCBs) of used cell phones (Ha et al. 2010). Li et al (2019) suggested at a macro level for the actual situation of each geographical region, the dismantling capacity of each region needs to be optimized according to the distribution of used cell phones in each region of China (Jiawen Li et al. 2019). A devise for automatic disassembly and recovery of CPUs from cell phone circuit boards based on machine vision is presented for the problem of disassembly and recovery of used cell phone circuit boards. At last, experiments demonstrate that the device can achieve stable and reliable disassembly and recovery of CPUs (He et al. 2020). The different activities related to the end-of-life process (together with the disassembly process) have been extensively studied and the information flow between the different stages of handling used products has been identified and used to develop the disassembly process models (Mehmet I. et al 2013) . Assembling recycled cell phone batteries, solar panels and light-emitting diodes for

lighting work can replace candles and provide quality and green lighting in remote and poor areas (Diouf, Pode, and Osei 2015) .

If there is a valuable part of the used cell phone to be recycled, it needs to be disassembled first. For example, for the PCB board, battery, screws, body of the used cell phone, the same recycling method cannot be used. A common method is to shred those equipment into particles that are usually less than 10 mm or less than 5 mm. The common processes used in processing fine particles of recyclables are Eddy Current Separation, Corona Electrostatic Separation and Jigging (Cui and Forssberg 2003). For example, the PCB board recycling method is generally used to crush the method after the chemical leaching method to extract the metal elements. After the initial shredding of the PCBs, a corona electrostatic separator is used to sort the shredded particles according to their material for further processing (Jia Li et al. 2007) .

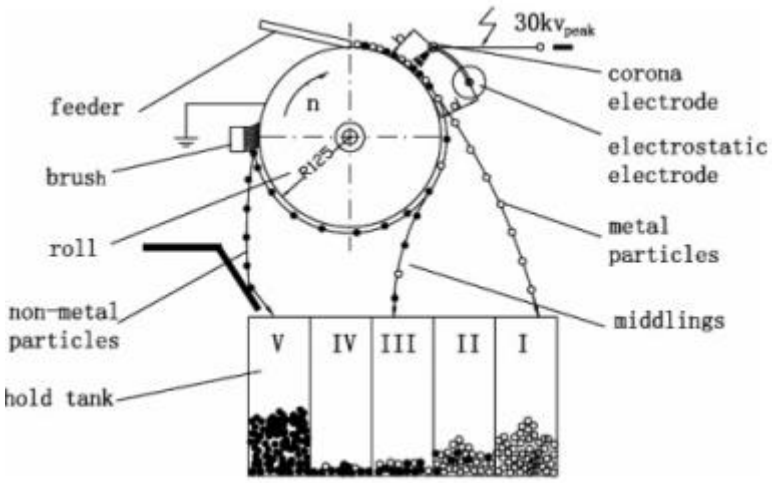


*Figure 3.2- Diagram of corona electrostatic separator (Jia Li et al. 2007)*

But nowadays it is usually a manual operation to remove PCBs from electronic devices. Not only for PCBs, disassembling screws and other small parts also requires manual operation to complete. Some researchers are currently studying how to use robots in the engineering field to complete part of the disassembly of electronic devices. From identifying the recycled objects to sorting, and later dismantling the phone screen and using robot arms with different end effectors to complete the dismantling of the phone, all can have different levels of robot involvement (Bogue 2019). It is also possible to work manually with the aid of a robot arm, replacing different types of screwdrivers to meet the work of unscrewing different types of screws (Chen, Wegener, and Dietrich 2014).

As it can be seen, it is valuable to study how to dismantle used cell phones in the engineering field, and this one link is a prerequisite for the subsequent link of recycling.

In practical terms, the use of robots to disassemble electronic devices has been successfully implemented by only a few companies because product information is more readily available to the manufacturers of these electronic devices (Foo, Kara, and Pagnucco 2022b). For example, the installation dimensions of each component of a cell phone vary from manufacturer to manufacturer for different products, so if a robot for automated disassembly is desired for all or most makes and models of cell phones, a locating system is required.

## 3.2 Computer vison application

In order to make the automated cell phone disassembly robot able to meet the size of most, various brands and models of cell phones, it is obviously impractical to input all the dimensions of all parts of all models of cell phones into the system. Moreover, used phones are likely to be broken and deformed to varying degrees, so it is not possible to automatically disassemble them, even if the standard dimensions of all models are known.

Therefore, there is a need for a fast, accurate technology that can identify and locate individual parts of cell phones, and computer vision technology can meet this need.

The object detection is performed in real time by the camera mounted on the robot arm, and the object recognition is performed using convolutional neural network (Zhang et al. 2019). Take the example of screws in cell phones, there are many models, so the requirement for the computer vision applied is to be able to discern the small gap between the detected objects. This can be achieved by building a convolutional neural network with increased training time and samples of the model (Wang, Li, and Zhang 2019). In addition, because of the location of the screws being inspected in the phone's distribution, computer vision needs to be able to accurately identify screws in different poses, in different positions, and at different angles. This requires sufficient, significantly different data in the training set to ensure the accuracy of the recognition (Mangold et al. 2022).

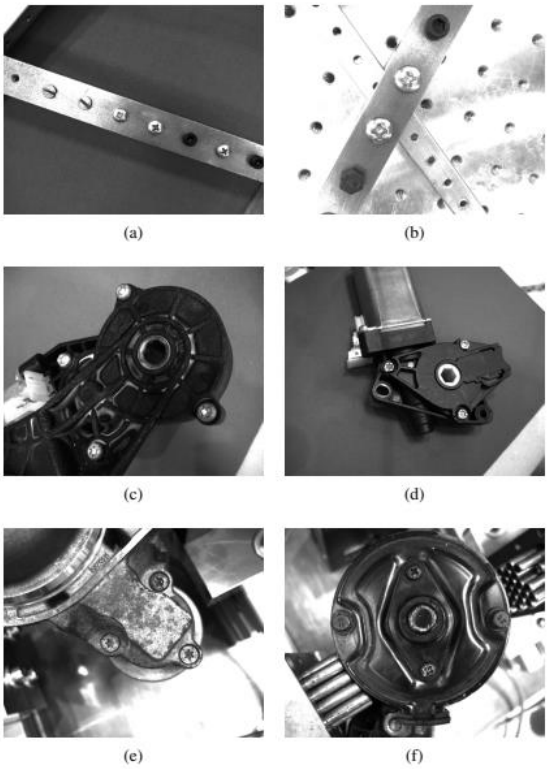


*Figure 3.3- Exemplary images of screws contained in the dataset (Mangold et al. 2022)*

Since the size of tiny parts such as screws used inside cell phones is very small, the application of computer vision requires a certain resolution of the camera and at the same time needs to consider the speed of recognition (Brogan, DiFilippo, and Jouaneh 2021). To solve the classification problem of various different types of screw heads, an architecture combining the Hough transform and a deep convolutional neural network is proposed (Yildiz and Wörgötter 2020). In the automated use of robots to recycle hard disk drives with many tiny parts inside, a combination of deep neural networks and point cloud processing is used to detect and identify the parts and screws in the drives (Yildiz et al. 2020).

The computer vision technology applied needs to be able to accomplish not only recognition, but also to locate the components within the used phone. A computer vision-based device for automatically disassembling and recycling CPUs on top of circuit boards inside used cell phones is proposed (He et al. 2020). It successfully identified and located CPUs on circuit boards covered with tiny parts. After calibrating the camera, the object can be positioned by the image taken by the camera (Farag, Ghafar, and Alsibai 2019). If computer vision is used to locate the battery inside the used phone, the size of the battery and the 3D coordinates of the feature points can be

determined based on the location of the marker points and reference lines after extracting the features to facilitate the next step of disassembly (Feng et al. 2017). Using a calibrated camera, a depth map is generated from the captured images and the 3D coordinates of the feature points are calculated, after which the control manipulator can pick up the specified items (Zhang et al. 2019). Ambrosch et al.(2018) present the results of research obtained during the development of a collaborative disassembly device for used cell phones, using computer vision technology to identify different models and to be able to proceed to the next step of disassembly. The possibilities of the latest automation technologies are demonstrated (Ambrosch et al. 2018). For different types of screws in different locations on the object, computer vision technology is used to identify and locate the screws and then automatically drive the matching screwdriver to unscrew them (Klas et al. 2021). Schumacher (2013) presents an automated method of battery disassembly, using computer vision technology to locate the battery and the actual disassembly work is carried out by the designed robotic arm equipped with different tool heads (Schumacher and Jouaneh 2013). But these examples of applying computer vision and manipulating robotic arms for automated disassembly tasks. There is no detailed explanation of why the serial manipulator is chosen, and other parts such as the camera used, the operating parameters of the manipulator, etc., are not demonstrated.

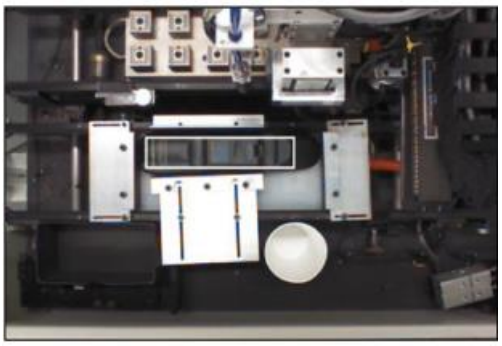

*Figure 3.4- Matched device image frame (Schumacher and Jouaneh 2013)*

Therefore, it is known that the use of computer vision technology can do the job of identification, positioning, and there are already some examples of using computer vision technology for picking up and disassembling parts by robotic arm. After using computer vision technology to identify and locate small parts, the manipulator can be driven to perform a series of subsequent disassembly

operations. There are many types of manipulators, and different manipulators can be selected according to different evaluation criteria.

## 3.3 Stewart Platform application

Stewart Platform is a kind of parallel manipulator, which has the characteristics of stability and high carrying capacity. And the reason for choosing Stewart Platform as the research object in this study is that since it is unknown how much force is needed to dismantle the screen or back cover of the used cell phone, the manipulator with high load-bearing capacity is firstly considered. Secondly, since removing the screws inside the used cell phone is also one of the important tasks, and Stewart Platform can satisfy the rotational movement in the horizontal plane, which can save the actuator of electric screwdriver if it is equipped with ratchet screwdriver.

In fact, the research on Stewart Platform has been relatively mature, and it can be applied in many fields to deal with a variety of different tasks. The use of parallel manipulators in various fields has become more and more evident over time and is widely used in precision manufacturing and medicine (Patel and George 2012). The Stewart Platform can be used to perform tasks that require the utmost precision, such as in the medical field where it can be used to perform neurosurgical surgery on patients. This requires the accuracy of the Stewart Platform to be very high and it must be very stable (Wapler et al. 2003). The Stewart Platform is available in sizes ranging from 130 mm to 3 m, with load capacities ranging from 0.5 to 1500 kg, vibration isolation and precise positioning are the two main indicators when considering drive design (Anderson et al. 2004).

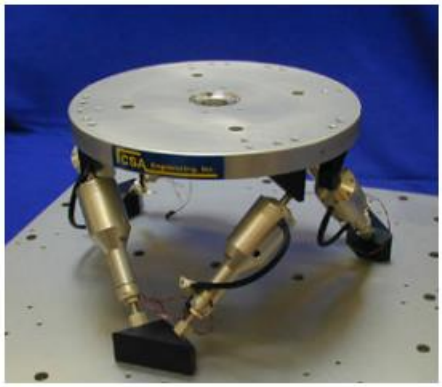

*Figure 3.5- A common Stewart Platform* (Anderson et al. 2004)

(Virgil Petrescu et al. 2018) present several main elements of the Stewart Platform, an accurate and original analytical geometric method is proposed to calculate the dynamical model and to calculate the individual parameters of the platform while performing the motion. (Kim et al. 2019) carry out the design of a typical Stewart Platform and later verified the accuracy and stability of the platform operation by monitoring the 3D coordinates of a total of 12 ball joints in the upper and lower planes. (Tang, Cao, and Yu 2019) design a Stewart Platform based on a voice coil motor and later perform experimental tests on this prototype to verify the vibration attenuation performance of the dispersion system. (Short et al. 2017) present a Stewart Platform for desktop assistance, with the main purpose of interacting and emotionally communicating with people, but also with applications in human health and education. When the stiffness of the surface on which the platform is placed is not uniform, the attachment stiffness above the Stewart Platform has a significant effect on the natural frequency of the entire platform (Ma et al. 2019). In order to design the Stewart Platform with high dexterity, (McCann and Dollar 2018) evaluated the effectiveness of the working space and the movement of the platform by considering both kinematic and tribomechanical aspects .

Although there are many types of Stewart Platform applied in various fields facing various work tasks, and they are relatively mature. However, since the main purpose of this study is to study disassembling cell phones, the Stewart Platform is only one aspect of it and not the main body of the study. Therefore, by reviewing this part of the literature, the main purpose is to have some understanding of the overall development findings and to be able to build a numerical model of the platform based on inverse kinematics. Since subsequent modeling work requires a theoretical basis, the next chapter ‘ theoretical framework’ will show the theoretical basis needed for modeling.

# 4 Theoretical framework

## 4.1 Coordinates transformation

As shown in Figure 4.1 as the Stewart Platform, there are six chains in a single structure that provide a parallel link between the output and base platforms, each with an active degree of freedom. The upper and lower platforms (the output platform and the base platform) are two arbitrary hexagons with a spherical kinematic sub attached to the vertices of the hexagon, which are then connected to each other by six extendable rods.

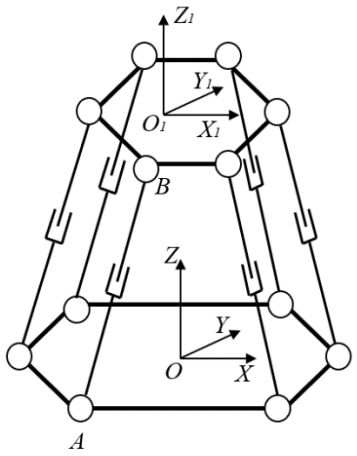


*Figure 4.1- Geometric model of Stewart Platform*

The $Z$ axis is perpendicular to the plane of the lower platform and the $Z_1$axis is perpendicular to the plane of the upper platform, and the coordinate system is established respectively. There are six joint points on both upper and lower platforms. Let the coordinates of the joint points on the upper platform be $(a_i\,,b_i)$ and let the coordinates of the joint points on the lower platform be $(c_i\,,d_i)$ in the coordinate system of the lower platform. In the $XYZ$ coordinate system of the lower platform, the coordinates of the joint points on the lower platform are $A_{oi}(a_i\,,b_i\,,0),i=1{\sim}6$, and in the $X_1Y_1Z_1$ coordinate system of the upper platform, the coordinates of the joint points on the upper platform are $B_1(c_i\,,d_i\,,0),,i=1{\sim}6$. The upper platform has 6 degrees of freedom in the process of motion, let the position parameters of the upper platform be $(x_c\,,y_c\,,z_c\,,\alpha\,,\beta,\gamma)$, $x_c\,,y_c\,,z_c$ are the coordinates of the center point of the upper platform in the $XYZ$ coordinate system, $,\alpha\,,\beta,\gamma$ are the angles of the rotation of the upper platform around $Z$axis, $Y$axis, $X$axis. The coordinates of the joint points on the upper

platform in the $XYZ$ coordinate system are $B_{oi}(x_i, y_i, z_i), i = 1{\sim}6$, which is shown in Figure 4.2.

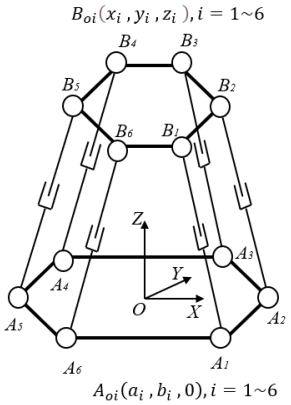


*Figure 4.2- The coordinates of ball joints in the $XYZ$ coordinate system*

$$B_{oi} = [M]B_{1i} \qquad (i = 1{\sim}6) \tag{1}$$

with

$$B_{oi} = (x_i, y_i, z_i)^T \tag{2}$$

$$B_{1i} = (c_i, d_i, 0)^T \tag{3}$$

$$[M] = \begin{bmatrix} \cos\alpha\cos\beta & -\sin\alpha\cos\beta & \sin\alpha & x_c \\ \sin\alpha\cos\gamma + \cos\alpha\sin\beta\sin\gamma & \cos\alpha\cos\gamma - \sin\alpha\sin\beta\sin\gamma & -\cos\beta\sin\gamma & y_c \\ \sin\alpha\sin\gamma - \cos\alpha\sin\beta\cos\gamma & \cos\alpha\sin\gamma + \sin\alpha\sin\beta\cos\gamma & \cos\beta\cos\gamma & z_c \\ 0 & 0 & 0 & 1 \end{bmatrix} = \begin{bmatrix} M_1 \\ M_2 \\ M_3 \\ 1 \end{bmatrix} \tag{4}$$

in which $M_1$, $M_2$, $M_3$ are the row matrixes consisting of the first row, the second row, and the third row in $M$.

## 4.2 Length of links and Derivation of Jacobian matrix

Once the coordinate conversion is completed, the coordinates of the points in the different coordinate systems are unified in the $XYZ$ coordinate system. After that, the length of each link can be calculated by using the coordinates of the upper platform and the coordinates of the lower platform.

$$d_i = [(x_i - a_i)^2 + (y_i - b_i)^2 + z_i{}^2]^{\frac{1}{2}} \tag{5}$$

The length of each link is $d_i$, which should be the function of $(x_c, y_c, z_c, \alpha, \beta, \gamma)$. The derivative of each of these 6 parameters is then written in matrix form to get:

$$d_i = \left[\frac{\partial d_i}{\partial x_c} \ \frac{\partial d_i}{\partial y_c} \ \frac{\partial d_i}{\partial z_c} \ \frac{\partial d_i}{\partial \gamma} \ \frac{\partial d_i}{\partial \beta} \ \frac{\partial d_i}{\partial \alpha}\right]\left(\dot{x}_c, \dot{y}_c, \dot{z}_c, \dot{\gamma}, \dot{\beta}, \dot{\alpha}\right)^T \ (i = 1\sim6) \tag{6}$$

$\dot{x}_c, \dot{y}_c, \dot{z}_c$ are the speed of the center of upper platform among $X, Y, Z$ axes. $\dot{\gamma}, \dot{\beta}, \dot{\alpha}$ are the angular speed of the upper platform around $X, Y, Z$ axes.

It could be expanded as:

$$\begin{bmatrix} \dot{d}_1 \\ \dot{d}_2 \\ \vdots \\ \dot{d}_6 \end{bmatrix} = \begin{bmatrix} \frac{\partial d_1}{\partial x_c} & \frac{\partial d_1}{\partial y_c} & \cdots & \frac{\partial d_1}{\partial \alpha} \\ \frac{\partial d_2}{\partial x_c} & \frac{\partial d_2}{\partial y_c} & \cdots & \frac{\partial d_2}{\partial \alpha} \\ \vdots & \vdots & & \vdots \\ \frac{\partial d_6}{\partial x_c} & \frac{\partial d_6}{\partial y_c} & \cdots & \frac{\partial d_6}{\partial \alpha} \end{bmatrix} \begin{bmatrix} v_x \\ v_y \\ \vdots \\ \omega_z \end{bmatrix} \tag{7}$$

Which equals to:

$$\dot{D} = [A]\dot{x} \tag{8}$$

If $[A]$ is invertible, then

$$\dot{x} = [A]^{-1}\dot{D} \tag{9}$$

$$A_{i1} = \frac{\partial d_i}{\partial x_c} = \frac{\partial d_i}{\partial x_i} \cdot \frac{\partial x_i}{\partial x_c} = \frac{x_i - a_i}{[(x_i - a_i)^2 + (y_i - b_i)^2 + z_i{}^2]^{\frac{1}{2}}} \cdot 1 = l_i \tag{10}$$

$$A_{i2} = \frac{\partial d_i}{\partial y_c} = m_i \tag{11}$$

$$A_{i3} = \frac{\partial d_i}{\partial z_c} = n_i \tag{12}$$

$$A_{i4} = \frac{\partial d_i}{\partial \gamma} = (l_i\,, m_i\,, n_i) \cdot \frac{\partial [M]}{\partial \gamma} \cdot B_{1i} \tag{13}$$

$$A_{i5} = \frac{\partial d_i}{\partial \beta} = (l_i\,, m_i\,, n_i) \cdot \frac{\partial [M]}{\partial \beta} \cdot B_{1i} \tag{14}$$

$$A_{i6} = \frac{\partial d_i}{\partial \alpha} = (l_i\,, m_i\,, n_i) \cdot \frac{\partial [M]}{\partial \alpha} \cdot B_{1i} \tag{15}$$

Therefore, $A_{ij}\ (i, j = 1{\sim}6)$ could fulfill the $[A]$

$$[J\,] = [A]^{-1} \tag{16}$$

After obtaining all the elements in the $[A]$, the definition of the inverse matrix leads to all the elements in $[A]^{-1}$. This gives us the Jacobian matrix $[J\,]$ , which enables the calculation of the velocity of the upper platform in six degrees of freedom.

# 5 Experiments

From the previous section, it is known that if the feasibility of the model is to be verified, the maximum tensile force that occurs during the disassembly of the phone screen needs to be measured, and then the maximum force that needs to be provided by each rod of the Stewart Platform is calculated so that the feasibility of the design solution can be verified. Therefore, this part needs to be measured experimentally.

## 5.1 Experiments design

The goal of the experiment is to measure the maximum tensile force required during the disassembly of a cell phone screen. In order to fix the sample to the equipment, a suitable fixture is selected. The purpose of the fixture is to limit the movement of the sample so that it does not become detached from the experimental equipment during the disassembly of the screen and so that the working parts of the fixture do not get stuck in the screen.

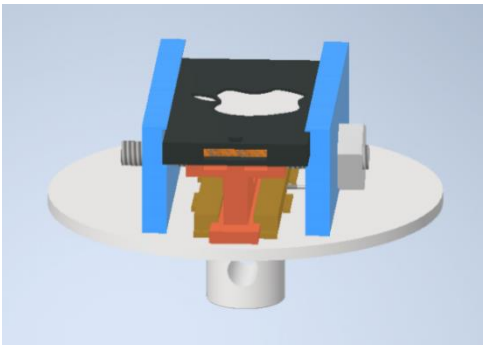

*Figure 5.1- The 3D model of the jig*

For these two factors, the fixture shown in the figure 5.1 is designed first. The lower end of this fixture can be assembled with the fixed end of the tensile machine, and the friction force can also limit the displacement of the sample in the vertical direction during disassembly. However, in the subsequent work, it is found that this fixture is not only complicated to assemble, but also the friction force is not sufficient to limit the displacement of the sample.

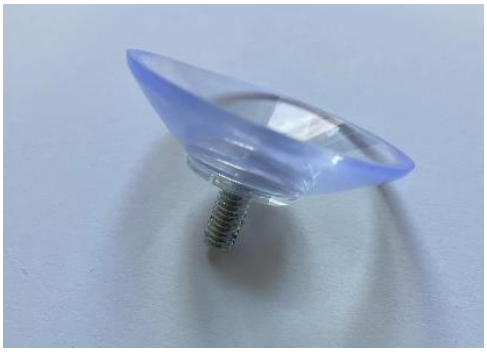

*Figure 5.2- The suction cup with a screw*

Since both the screen and the back cover of the sample had smooth surfaces, the phone screen is subsequently removed using a suction cup with a screw on one end as shown in the figure 5.2. This is easy to install and also ensures that no displacement occurs.

The glue used for gluing between the screen of the phone and the main body of the phone, the glue will melt when the temperature rises, so the experimental temperature can also be used as one of the independent variables, the purpose is if by changing the temperature can reduce the maximum force needed in the process of disassembling the screen phone, that is, the experiment can plot the curve between force and temperature, and then find the optimal working temperature. However, due to the limited experimental samples, this part can be used as FUTURE WORK. The main purpose of this experiment is only for the maximum force required to disassemble the phone screen, and if the temperature increases, the maximum force will be reduced, the maximum force measured at room temperature already includes this situation. The maximum force measured at room temperature is already included in this case. If it can meet the working requirements at room temperature, it can also be met at elevated temperature.

When using an existing tensile machine to disassemble a cell phone screen, it is also possible to set the speed of movement of the moving part above, without knowing whether this will have an effect on the measured maximum tensile force. If there is a correlation between the disassembly speed and the maximum pulling force, the working speed of the proposed solution needs to be set, and therefore needs to be taken into consideration.

Since the maximum recommended storage temperature for iPhone is 45 ℃, higher than 45 ℃ may cause battery failure, and the maximum movement speed of the existing tensile machine is

10mm/s. In order to measure the maximum force generated by disassembling the cell phone screen and to verify the correlation between the maximum force and temperature and speed, the experimental samples are divided into three groups with speeds of 1mm/s, 5mm/s, and 10mm/s. In each group, three different operating temperatures are set: room temperature (22 ℃), 40 ℃ (for experimental safety reasons), and 30 ℃. In each speed group, the majority of the samples are measured at room temperature.

According to the experimental expectation, if the final data show that the data with the same velocity and temperature are normally distributed, then the experimental expectation is met. Using the 6sigma method, the maximum force is calculated by calculating the mean and variance if it satisfies u+6sigma, it means that there is 99.999997% probability that this maximum force can successfully satisfy the work under this independent variable condition requirements. The following processing and calculation of the experimental data will be described in detail in the corresponding sections.

## 5.2 Detailed procedure of the experiments

The experiments are conducted on the basis of an existing stretching machine, which is divided into a moving part above and a fixed part below, both of which have clamps to hold the device tightly for disassembly. In the fixed part below, a suction cup with a screw at one end is used to hold the phone. The screw part is clamped with a jig and the sample is placed on the suction cup and pressed so that the suction cup can firmly hold the back cover of the phone. The same suction cup with a screw at one end is used for the upper moving part and the screw is clamped by the fixture. The upper moving part is controlled to move downward so that the suction cup presses on the sample. After that, the experiment was performed and the screen was pulled apart when the moving part was moved upwards. The maximum force that occurs during the process is recorded. First, the samples are marked to observe whether the screen is broken or not, and there are some cell phones with different degrees of screen breakage. For these phones with broken screens, if the phone screen is continued to be disassembled according to the previous method, the disassembly is likely to fail due to the poor suction cup suction.

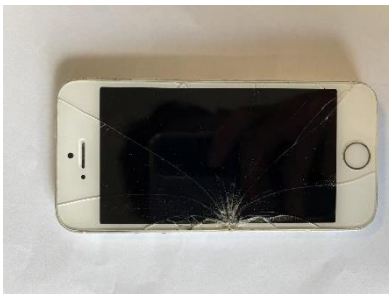

*Figure 5.3- No.4 sample. One side of the screen is visibly cracked*

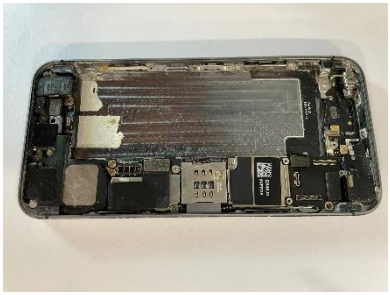

*Figure 5.4- No.21 sample. Reassemble with glue, tested twice to success*

*Figure 5.5- No.22 sample. The 'Home' key is off and the edge of the screen is cocked up*

*Figure 5.6- No.23 sample. The edges of the screen have obvious gaps and are seriously aged*

*Figure 5.7- No.31 sample. The screen is surrounded by visible cracks.*

Also for experimental safety reasons, for cell phones with broken screens (also including the location of the suction cups sucking hard to remove stains, resulting in uneven surfaces so that the suction cups do not suck firmly), put a layer of transparent tape on the phone screen flat and wrinkle-free, and keep the surface smooth.

*Figure 5.8- Using suction cups to dismantle screens of phones*

A tensile machine with an oven is used to conduct the experiment so that the temperature conditions for disassembling the phone could be guaranteed.

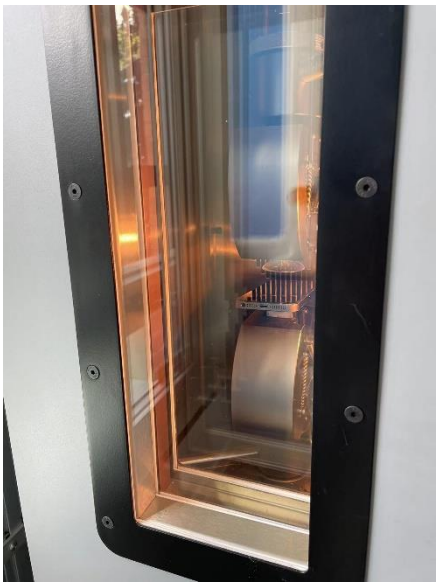

*Figure 5.9- Using the oven to control the temperature of phone screen removal*

The experimental samples included 7 iPhone 4, 36 iPhone 5, 10 iPhone 5C, 6 iPhone 6 and 1 iPhone 6 plus. First, the two fixing screws on the bottom of the phone are removed manually using an adapted screwdriver, after which the experiment started at room temperature (22 ℃). Since the number of individual phone models is limited, some models have too little data for data analysis if the effects of temperature and speed are considered for each model. Therefore, only the largest number of iPhone 5 is selected for experiments concerning temperature and speed, and all other models are disassembled at room temperature only.

# 6 Result and analysis

## 6.1 3D model

The working space of the compliant Stewart Platform needs to be determined based on the length, width, and height of the iPhone available. An example of a Stewart Platform that can meet the requirements, references for preliminary modeling (M. H. Khamsehei Fadaei et al. 2017). The whole Stewart Platform can be simplified into four parts: base, end effector, down piston, and up piston, where the end of the down piston is connected to the base by a ball joint, the connection between the up piston and the end effector by a ball joint, and the connection between the down

piston and the up piston by a ball joint.

In fact, the joints of the Stewart Platform should be created separately, but this part is not strongly related to the objective of this thesis, and the subsequent work is mainly to study the length of each rod, so these joints are simplified.

The dimensions of each part of the model are as follows.

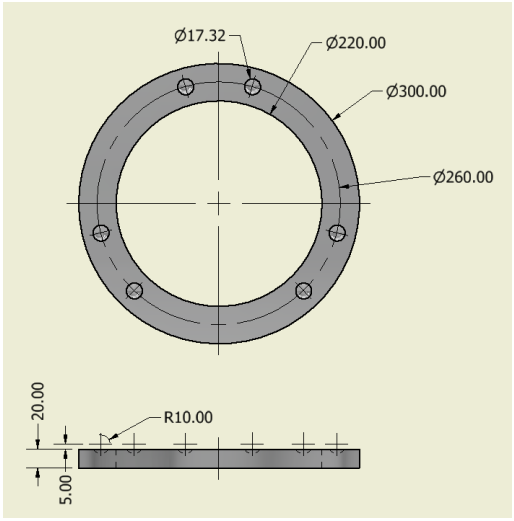


*Figure 6.1- Dimensions of the base*

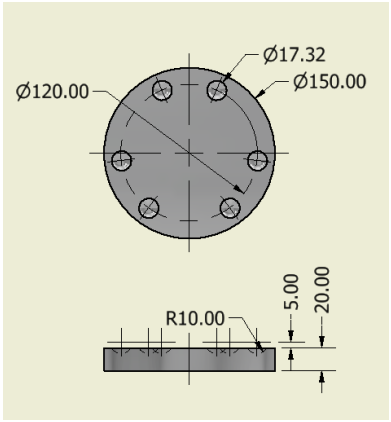


*Figure 6.2- Dimensions of the end effector*

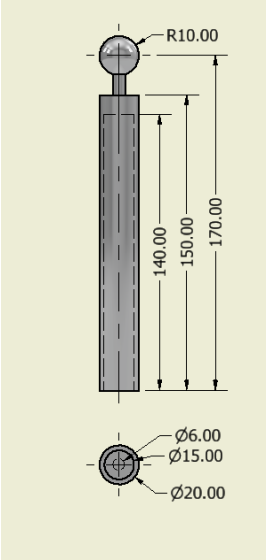


*Figure 6.3- Dimensions of the lower pistons*

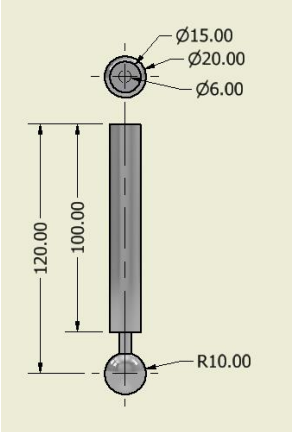


*Figure 6.4- Dimensions of the upper pistons*

After the model is created, it is possible to visualize how the proposed Stewart Platform works for the disassembly of used cell phones. Stewart Platform has a fixed base and the end effector is parallel to the base and can move in all directions in space. On top of this, the end effector can also rotate around the $Z$ axis at an angle, which can be used to remove the screws.

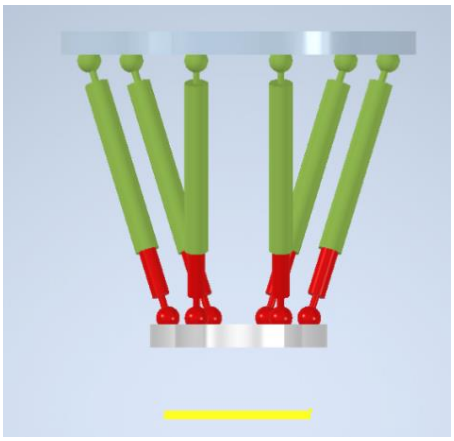

*Figure 6.5- The Stewart Platform working model schematic*

In the Figure 6.5, it can be visually seen that the end effector can move up and down in translation along the $Z$ axis. When the phone is fixed on a flat surface using some kind of fixture, the end effector is equipped with a suction cup, which is used to remove the screen of the phone. In this process, the elongation of the six rods of the whole Stewart Platform is always the same.

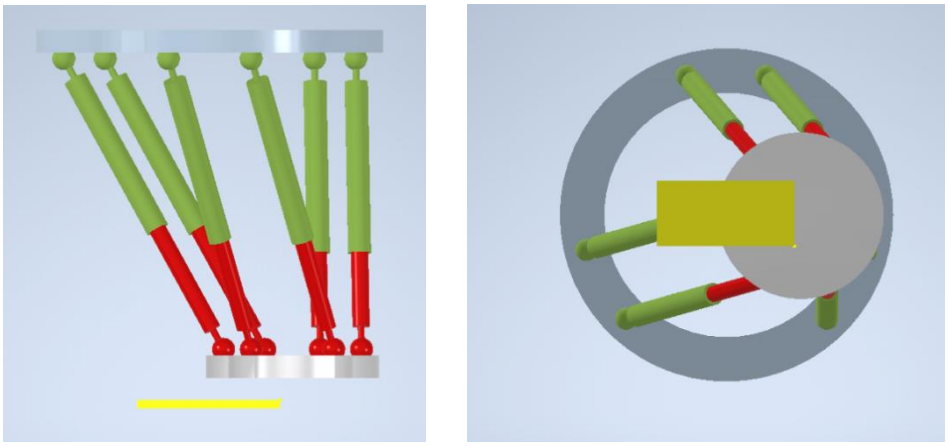

*(a) From the front* *(b) From the bottom*

*Figure 6.6- Schematic diagram of the Stewart Platform working at the edge of the phone*

At the end of the disassembly work, the disassembled parts are placed in a fixed position next to each other by controlling the translational movement of the end effector in the $X-Y$ plane. After opening the screen of the phone, the exposed screws are inside the phone. In this part, the computer vision technology mentioned in the previous 'literature review' will be usefel to identify and locate the screw heads and select the appropriate screwdriver for disassembly. When

removing these screws, the end effector is equipped with an adapted ratchet screwdriver with a magnetic screwdriver head, and the screws are unscrewed by continuously rotating and resetting the end effector around the $Z$ axis in one direction. This eliminates the need to equip the screwdriver with an additional motor. After the screw has been removed, the end effector moves to a fixed position and places the removed screw in place.

In order to verify the viability of the solution during the removal of the phone screen and screws, it is necessary to find the maximum force that occurs during the removal process in order to calculate the maximum force that needs to be provided by the motor on the rod of the Stewart Platform. The following study will investigate the maximum force generated in the process of removing the screen of the phone.

## 6.2 Digital model in Simulink

The finished model is first exported to a file format that can be read by Simscape in MATLAB, and then the model file is imported in MATLAB. The generated Simulink module contains the joints and solids corresponding to the model. The assembly between these modules is done by coordinate transformation.

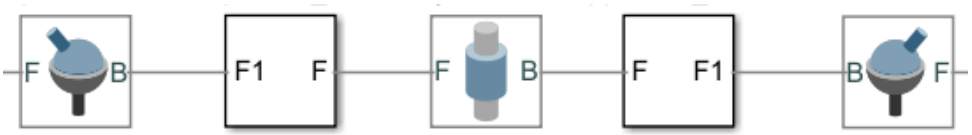


*Figure 6.7- The solids and joints in Simulink*

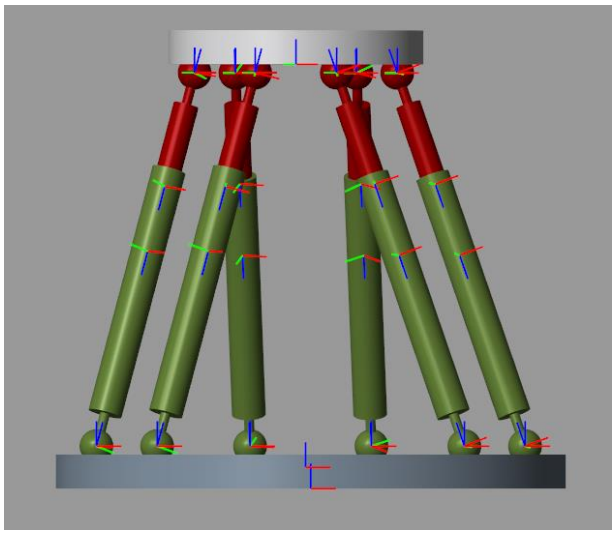

*Figure 6.8- The preview of the model in Simulink*

In order to control the model so that the Stewart Platform can translate in any direction and rotate about each axis, six degrees of freedom are required. Therefore, according to the theoretical model in the previous section, the code is written to calculate the rod length of each of the six pistons, given the position and posture of the end effector.

To verify that the model can move according to the given signal, the position and posture of the end effector need to be calculated at all times, and the length of each piston needs to be calculated afterwards. This calculation process consists of two parts, the first part serves to input a continuous signal and output six variables to determine the position and posture, the second part is to calculate the length of each piston based on the position and posture.

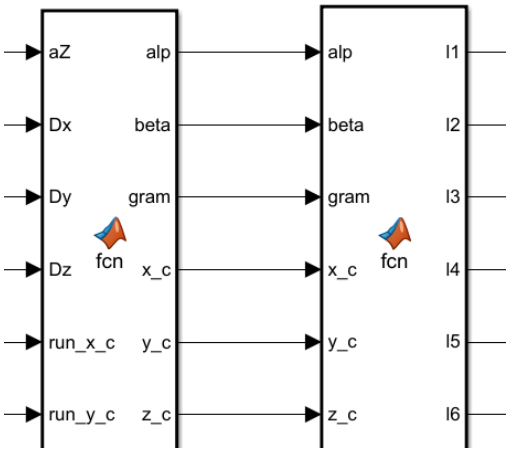


*Figure 6.9- The functions for calculation in Simulink*

Assuming that the initial state of each piston is without any displacement, the initial length is

measured to be 190 mm, after which the displacement of the prismatic joint in the $Z$ axis direction is the elongation of the piston for the purpose of the subsequent PID part. Therefore, after calculating the length of each piston, the initial length should be subtracted.

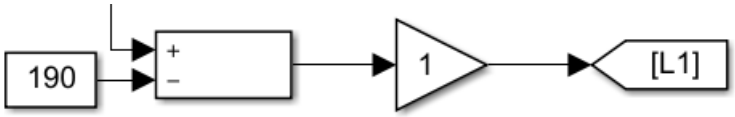


*Figure 6.10- Minus the initial length*

Set the coordinate system where the base is located as the reference coordinate system of the whole Stewart Platform, transform the coordinates of the end effector into the coordinates under the reference coordinate system, and output the 3D coordinates to verify the correctness of the Simulink model.

During the implementation of the Simulink model, each piston needs to be configured to be able to achieve the feedback effect of the end effector position on the rod length. Inside the "Prismatic" module, the actuation has "motion" and "force", "motion" will be calculated automatically, and "force" is provided by the PID module; sensing picks "position" to detect the position of the prismatic joint at all times. The PID module has two inputs, the rod length and the coordinates of the prismatic joint on the $Z$ axis; and one output, which is used to actuate the prismatic joint.

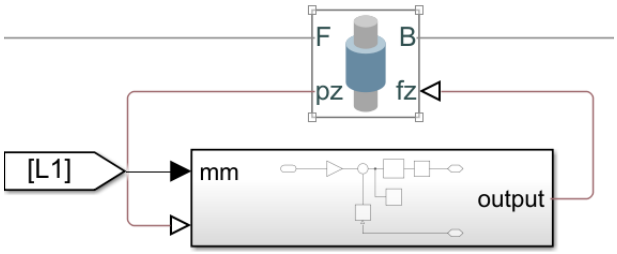


*Figure 6.11- Control of joints by PID*

Set the end effector to x=0 and z=250. The input signal in the x-direction is a sine function of amplitude 10. The expected motion should be, along the y-axis. Observe the actual motion of the end effector compared to the input as follows.

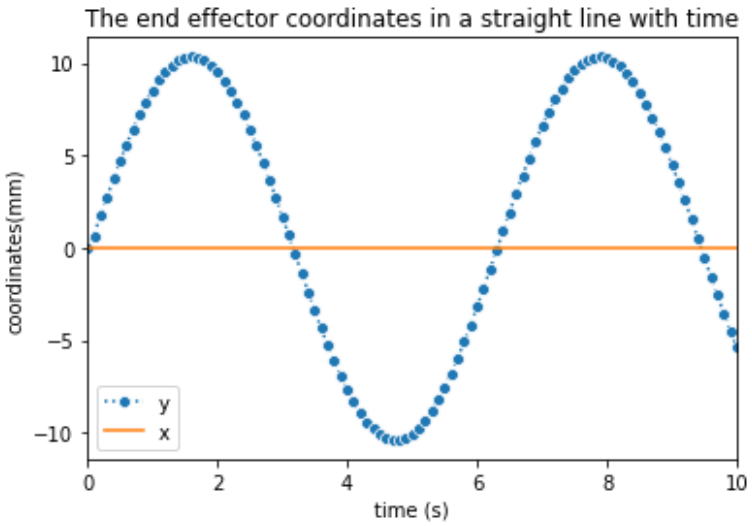


*Figure 6.12- The x and y coordinates of the end effector doing linear motion*

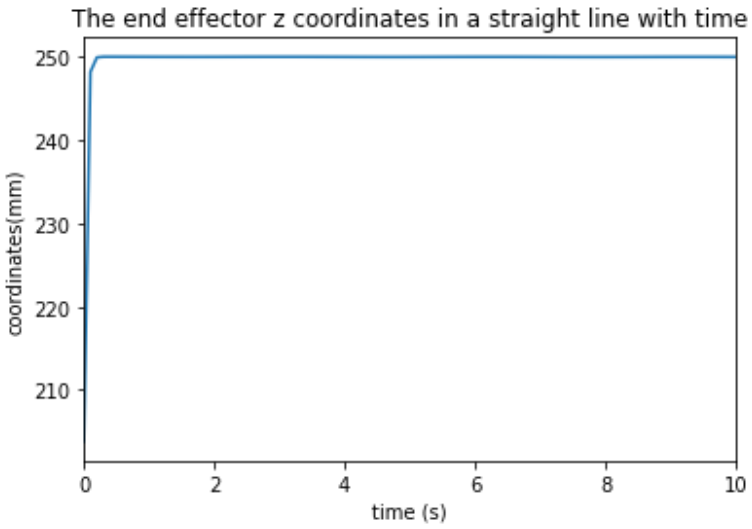


*Figure 6.13- The z coordinate of the end effector doing linear motion*

The $x, y, z$ coordinates of the end effector are shown in Figure 6.12 and 6.13. As the time changes from 0 to 10 seconds, the $y$ coordinate changes as a sinusoidal function of amplitude 10, the $x$ coordinate stays at 0, the $z$ coordinate rapidly grows from 0 to 250mm and keeps staying.

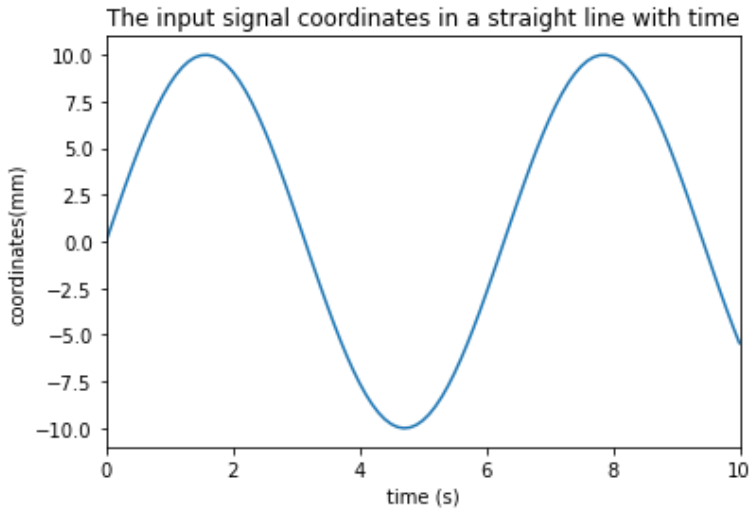


*Figure 6.14- The input y coordinate*

The input signal on the y-axis is shown in the Figure 6.14 as a sine curve. From the Figure 6.12, 6.13, 6.14, it can be clearly observed that the end effector has a height of 250 mm in the $Z$ axis direction, which is consistent with the setting. The displacement in the $X$ axis direction is zero, which is consistent with the setting. The output of the end effector in the $Y$ axis direction is consistent with the input signal, which is a sine wave with an amplitude of 10.

During the motion, the length of each piston varies as shown below.

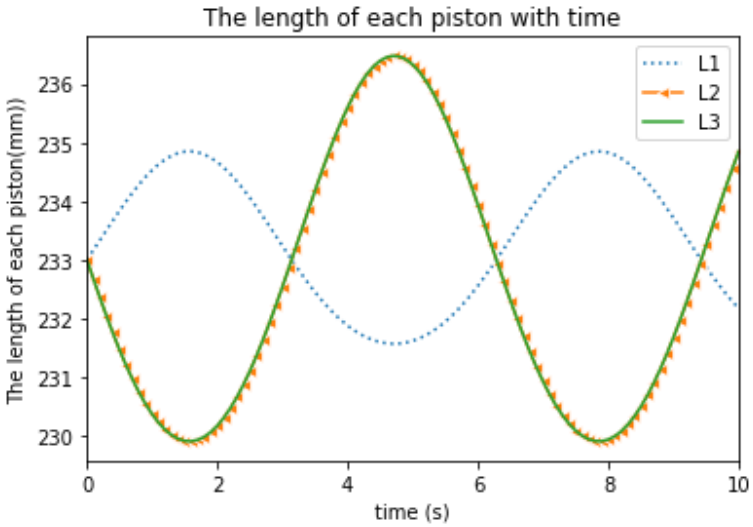


*Figure 6.15- The length of L1, L2 and L3 when the end effector doing linear motion*

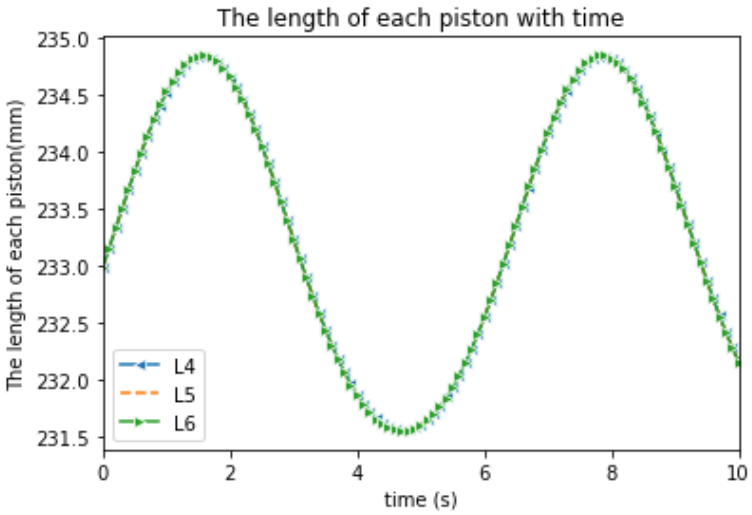


*Figure 6.16- The length of L4, L5 and L6 when the end effector doing linear motion*

When the end effector moves in a straight line, the length of each rod changes as shown in Figure 6.15 and Figure 6.16. The lengths of L1, L4, L5, and L6 have the same variation with a sinusoidal trend and a standard value of 233 mm with an amplitude of about 1.6. The lengths of L2 and L3 have the same variation with an amplitude of about 3.2.

To verify the effect of the model simulation, the end effector is controlled to move along a circular trajectory on the plane, and the final coordinate change is compared with the input signal.

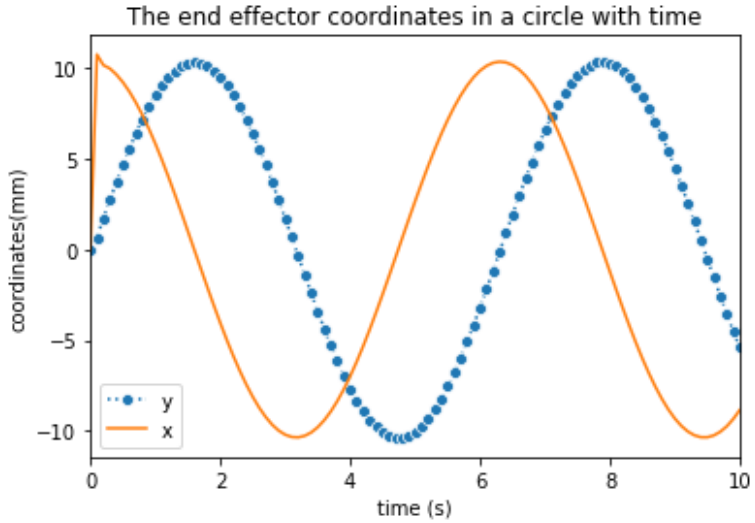


*Figure 6.17- The x, y coordinates of the end effector doing circular motion*

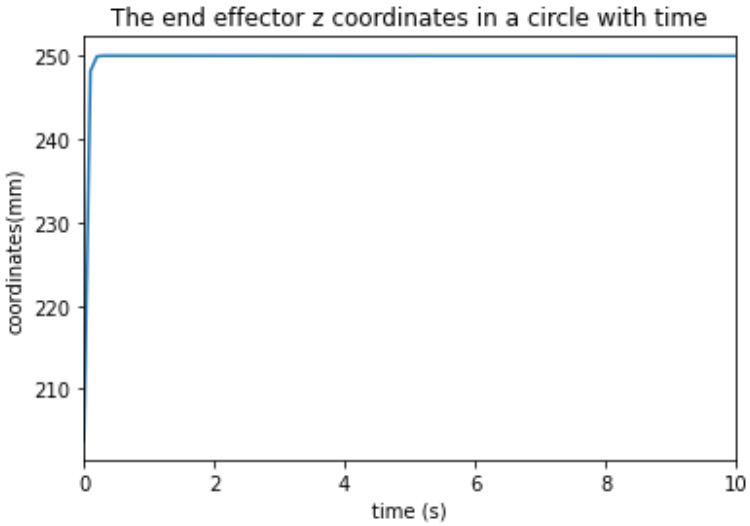


*Figure 6.18- The z coordinate of the end effector doing circular motion*

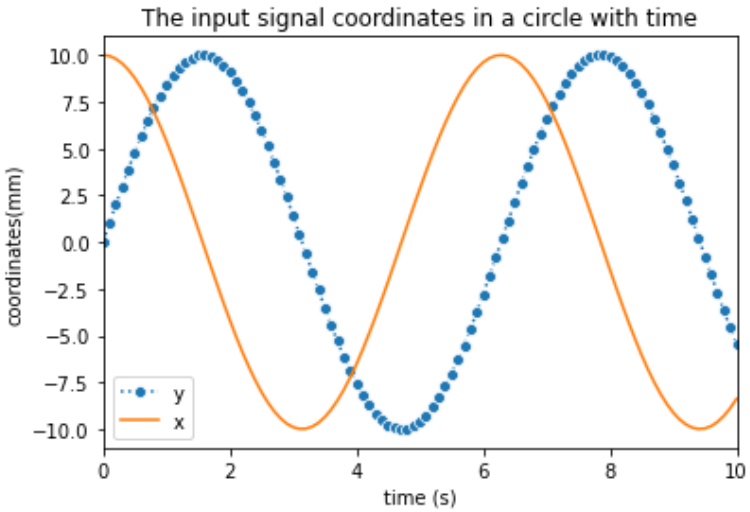


*Figure 6.19- The x, y coordinates of the input signal*

The $z$ coordinate of the set plane of motion is 250mm. The z coordinate of the end effector increases rapidly from 0 to 250mm in Figure 6.18. Comparing Figure 6.17 and Figure 6.19, the $x$ and $y$ coordinates are consistent, with $x$ varying as a cosine function curve and $y$ varying as a sine function curve, both with an amplitude of 10.

The length of the six pistons during the motion along the circular trajectory is shown in the figure below.

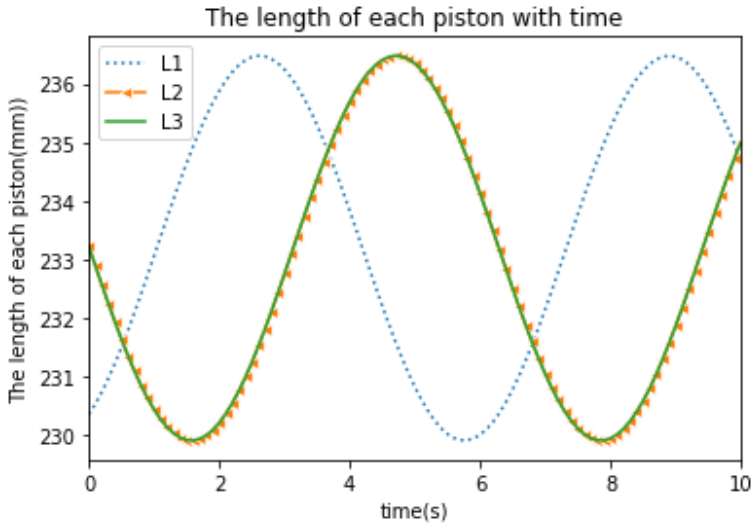


*Figure 6.20- The length of L1, L2 and L3 piston when the end effector doing circular motion*

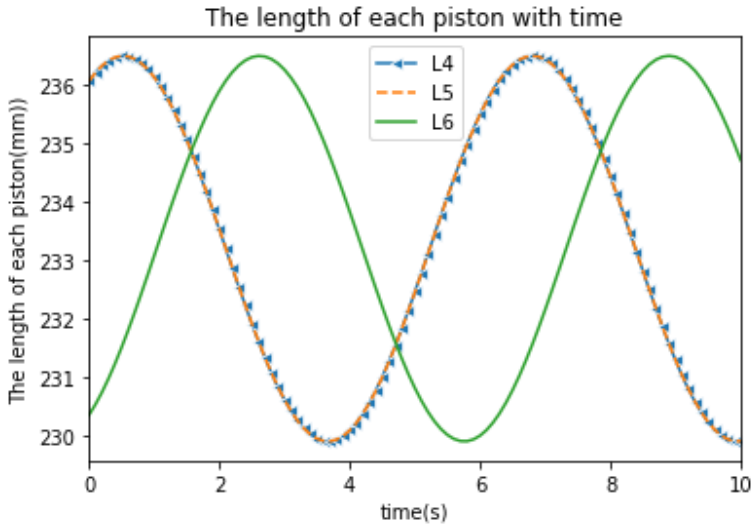


*Figure 6.21- The length of L4, L5 and L6 piston when the end effector doing circular motion*

In Fig. 6.20 and Fig. 6.21, it is obvious that when the trajectory of the end effector is a circle in the horizontal plane, L1 and L6 vary the same, L2 and L3 are the same, L4 and L5 are the same, and the period and amplitude of each set of curves are the same.

In order to meet the working requirements, it is therefore necessary to verify if the kinematic stage of the model can be rotated around the $Z$ axis at the given x and y coordinates within the working range, as required. Since one of the target effects moves in such a way that the end effector rotates around the $Z$ axis. After setting the rotation angle in the simulation, the result is shown in the Figure 6.22 that follows.

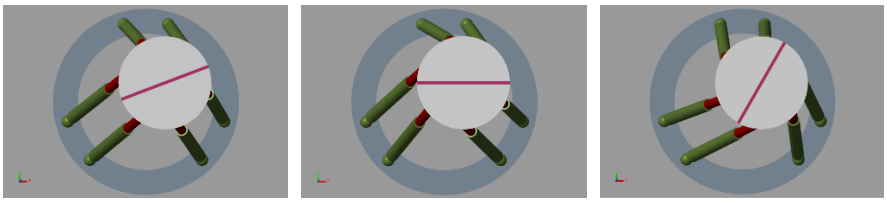

*Figure 6.22- The effect of the end effector doing rotation around z axis*

## 6.3 Analysis

The results of the experiment show that there are 59 experimental samples, of which two iPhone 5 disassembly failed and the rest measured values. Those two samples (19,26) failed to disassemble because the back cover of the phone is too uneven, causing the suction cups placed in the lower part of the pulling machine to fail to hold. Since the type of experiment is destructive, only one experiment can be done for each sample.

First, the maximum force required to remove the iPhone 5 screen is measured for the largest number of samples. Since it could not be determined whether temperature and speed had an effect on the experimental results, the Shapiro-Wilk test should first be performed separately from the data at the same experimental temperature and speed to verify whether the data are naturally distributed.

**The maximum force required to dismantle the iPhone 5 screens at different temperatures and different speeds. Unit(N)**

| Temperature(°C) | 1mm/s | 5mm/s | 10mm/s |
|---|---|---|---|
| *22* | *41.44* | *38.81* | *37.87* |
| *22* | *40.23* | *39.81* | *43.05* |
| *22* | *40.13* | *41.8* | *42.85* |
| *22* | *39.93* | *41.35* | *36.00* |
| *22* | *39.82* | *39.73* | *40.79* |
| *22* | *41.83* | *40.81* | *44.14* |
| *22* | *42.51* | *38.66* | |
| *30* | *31.71* | *28.43* | *27.36* |
| *30* | *26.48* | *31.09* | *32.34* |
| *40* | *23.53* | *22.79* | *20.60* |

Because of the sample size, the number of samples at 22 ℃ is sufficient, and the Shapiro-Wilk test ($\alpha = 0.05$) is performed separately for data that are at each speed. The null hypothesis for this test is that the overall distribution is normal. As a result, if $p < \alpha$, the original hypothesis is rejected

and there is evidence that the data tested are not normally distributed. On the opposite hand, if $p > \alpha$, the original hypothesis cannot be rejected (the data is from a normally distributed population).

**The results of the Shapiro-Wilk test are carried out on the experimental data obtained at different speeds under 22℃**

| Speed | Test statistic | p-value |
|---|---|---|
| *1mm/s* | *0.86385* | *0.16386*$> 0.05$ |
| *5mm/s* | *0.93057* | *0.55574*$> 0.05$ |
| *10mm/s* | *0.90678* | *0.41556*$> 0.05$ |

Therefore, the data for 22°C at 1mm/s, 5mm/s, 10mm/s is normally distributed. After that it is necessary to verify that the rest of the data is naturally distributed and to verify if temperature and speed affect the maximum force required to remove the phone screen. Because of the presence of two independent variables, the analysis is performed using ANOVA. The results of experiments with different speeds at the same temperature can be validated if the validation can conclude that the change in speed does not have a significant effect on the experimental results (the sample size will be sufficient for the Shapiro-Wilk test).

Observe the distribution of all data, Figure 6.23 shows the distribution of the maximum force required to disassemble the screens of the phones in different temperature and disassembling speed.

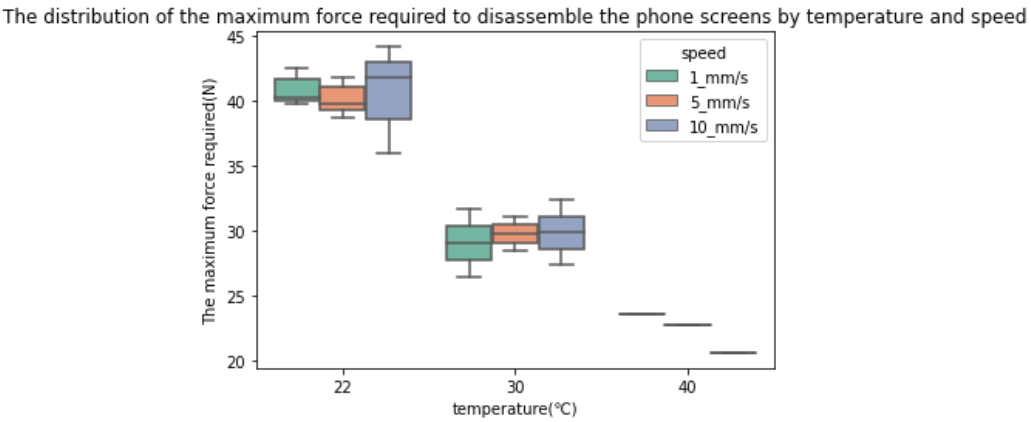


*Figure 6.23- The boxplot of the maximum force of disassembling screens*

To verify the effect of the interaction between temperature and speed when disassembling the phone screen, interaction plots are drawn for observation. It helps to visualize the mean values of the dependent variables at different temperatures and speeds on a single graph.

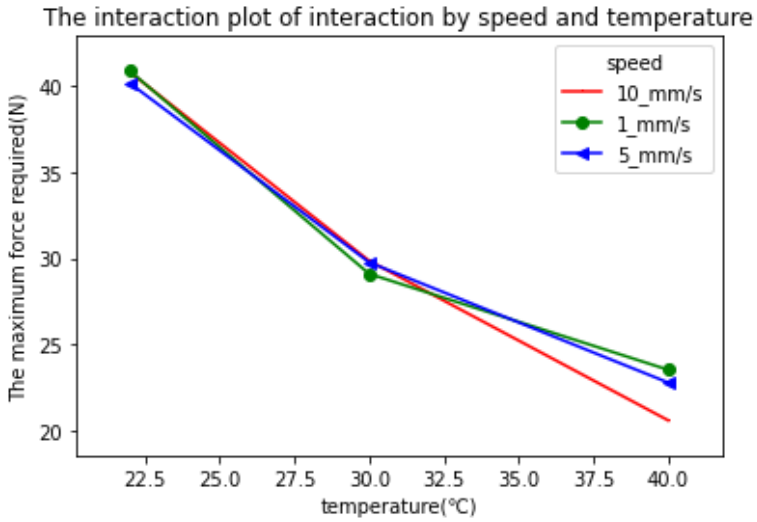


*Figure 6.24- The interaction plot of interaction by speed and temperature*

It can be visualized from the interaction diagram that the interaction between velocity and temperature is not significant, and the three lines appear to cross.

In order to verify, whether the difference in speed would have an effect on the maximum force generated during the disassembly of the phone under the same temperature conditions. Therefore, the experimental data obtained at different speeds at 22°C are subjected to ANOVA. If $p > 0.05$, the original hypothesis cannot be rejected, which equals to the speed doesn't influence the result of the maximum force. The result of the ANOVA is $p = 0.83013 > 0.05$, so the original hypothesis can be rejected.

**Shapiro-Wilk test results for all data measured at the same temperature**

| Temperature (℃) | Test statistic | p-value |
|---|---|---|
| *22* | *0.98158* | *0.95280*$> 0.05$ |
| *30* | *0.90071* | *0.37813*$> 0.05$ |
| *40* | *0.92453* | *0.46848*$> 0.05$ |

From the results of the Shapiro-Wilk test for all data measured at the same temperature, it is known that the original hypothesis cannot be rejected because the $p > 0.05$. This also shows that at 22℃, 30℃, 40℃, all the data fit a normal distribution.

# 7 Discussion

From the previous chapter, it is known that the maximum force required to dismantle a cell phone screen is related to the temperature at the time of dismantling. Among the three temperature control groups of 22°C, 30°C and 40°C, the average value of the maximum force required to disassemble the phone screen is the largest at 22°C. The main purpose of the experiment is to measure the maximum force required to disassemble the phone screen, so the data at room temperature is chosen for the next calculation. At 22°C, the data are normally distributed, so it can be calculated using Six Sigma (6σ).

A normal distribution is a distribution with two parameters, the first parameter $\mu$ is the mean of the random variable that follows the normal distribution, and the second parameter $\sigma$ is the standard deviation of this random variable. The probability rule for a random variable following the normal distribution is that the probability of taking a value near μ is large, while the probability of taking a value farther away from $\mu$ is small; the smaller $\sigma$ is, the more concentrated the distribution is near $\mu$, and the larger $\sigma$ is, the more dispersed the distribution is.

In the normal distribution curve presented by all data at 22°C, it is calculated that $\mu = 40.58N$ and $\sigma = 1.87N$. Therefore, it can be reasoned that there is a 99.9999997% probability that the maximum force required to disassemble the screen of a used iPhone 5 at 22°C is in the range of 29.36N($\mu - 6\sigma$) to 51.80N($\mu + 6\sigma$). In other words, if the iPhone 5 screen is successfully removed, there is a 99.9999997% probability that the maximum force generated in the process is between 29.36N and 51.80N. In order to further calculate the maximum force to be provided by each actuator, 51.80N is therefore chosen as a reference value.

When the end effector of the Stewart platform is in neutral position and the phone screen is disassembled, the length of all pistons is the same. When all pistons have 0mm elongation, the initial state is 190mm for each piston, and the distance of the end effector from the base on the $Z$ axis is 173mm. Then the cosine of the angle between each piston and $Z$ axis is 0.912. When all the pistons are 80mm long, they are in the limit of elongation, and the length of each piston is 270mm. the distance of the end effector from the base on the $Z$ axis is 258.87mm, and the cosine of the angle between each piston and the $Z$ axis is 0.959. Then it can be calculated that when the

end effector is in neutral position, the force provided by each piston with the same length (190mm) is also the same, 9.47N. The force provided by each piston with the same length (270mm) is 9.00N. At this point, the maximum force that needs to be provided by each actuator is calculated.

As mentioned in the previous 'Literature Review' section, if automated dismantling of cell phones is desired, the manufacturer of the cell phone can design the dismantling method for their own brand because they have all the parameters of the phone. However, if the dismantling process is to be effective for most models of used cell phones, there are more issues to be considered in the design phase, including the choice of the actuator to meet the requirements of the work. The actuators need to be able to offer enough force which is required during the process of disassembly work. Unfortunately, the various cell phone manufacturers do not publish the data that would help, such as the preload force of the mounting screws, the force needed to remove the phone screen, and the force needed to remove the battery. It is also possible that these manufacturers did not conduct the relevant tests. This thesis starts with the construction of a numerical model of the Stewart Platform, followed by a series of experiments using the iPhone as a sample to measure the maximum force required during the disassembly of the screen at different temperatures and speeds. After that, the iPhone 5 with the most samples at 22℃ is selected to calculate the maximum force required by each actuator of the Stewart Platform. Although this thesis may fill in some gaps, the validity of the final data is only limited for the disassembled iPhone 5 screen at 22°C because the relevant experiments performed are destructive and a sample can only be used once. In other words, if the application is to be applied on other models of used phones, it still needs to be tested first.

# 8 Conclusion

In this thesis, the initial goal is to design a system that could automate the dismantling of most types of used cell phones. To accomplish this goal, Firstly, the traditional way of cell phone recycling and now the new automated way of cell phone recycling are reviewed, after that the possibility of using computer vision technology and applying Stewart Platform to accomplish the goal is proposed. After that, a 3D model of Stewart Platform and a digital model in MATLAB using Simscape were built based on the theoretical basis of reverse dynamics. Afterwards, the feasibility of the digital model is verified, and the position of the end effector could be controlled to perform translational and rotational motions with the desired trajectory. Furthermore, experiments were conducted using a tensile machine to dismantle the iPhone screen, focusing on used iPhones and dividing them into different speed groups with different temperature combinations. The results of the experiment showed that there is a 99.9999997% probability that the maximum force required to disassemble the screen of a used iPhone 5 at 22°C is in the range of 29.36N to 51.80N. Further calculations showed that the maximum force required by each actuator in the Stewart Platform to disassemble the screen is 9.47N.

# 9 Future work

For the overall solution, there are still many details to consider. How to connect the cameras needed for the computer vision part and the end effector of the Stewart Platform, or how to arrange the cameras for detection and localization. Whether it is possible to use the same method for the disassembly of the phone screen for different assembly methods of used phones, which also corresponds to the use of different mounting clamps to fix the body. For the removal of parts on the horizontal plane, the calipers can be used for fixing (Schumacher and Jouaneh 2013). Moreover, if one Stewart Platform is used for all disassembly work, different end effectors such as suction cups, ratchet screwdrivers, etc. will be required. Therefore future work should consider

how to replace grippers and whether it is possible to use a Multi-functional gripper (Borras et al. 2018).

For the digital model of the Stewart platform, different optimization methods should correspond to different target objects for accomplishing different work tasks. For example, if the parts are not tightly coupled to each other, then the requirements for maximum forces during disassembly will be reduced accordingly. In this case, if the model is to be optimized, the requirements for load-bearing capacity will be reduced accordingly. The selection and optimization of dimensions and materials for each part of the model is also one of the future directions, but also in terms of the goals to be accomplished. In other words, before considering the optimization of the model, more research on the phone to be disassembled has to be done first.

This thesis focuses on the disassembly of iPhone 5, but according to the table in the appendix, although data from other iPhone models were also obtained, the number of samples is not enough if considering the division into temperature and speed groups for the next step of data analysis. However, a cursory observation shows that the maximum force required to remove the screen at the same temperature is very different for different phone models. Therefore, the experimental part of future work could focus on this point by comparing the disassembly process for different phone models and then having more specific requirements for the actuator of the Stewart platform used. Furthermore, although the focus of this thesis is on the maximum force during the disassembly of a cell phone screen, the material of the movable platform, the piston, the mass of the end effector and the camera (if the camera is on the movable platform) can also affect the results if a prototype is used for testing, as the self-weight can affect the requirements for the actuator.

# 10 Appendix

**The maximum force required in the process of removing the screen of the phone**

| No. | Type of iPhone | Temperature (℃) | Speed (mm/s) | Maximum force(N) |
|---|---|---|---|---|
| 1 | iPhone 5 | 22 | 1 | 41.44 |
| 2 | iPhone 4 | 22 | 5 | 13.84 |
| 3 | iPhone 6 | 22 | 1 | 8.58 |
| 4 | iPhone 5 | 22 | 1 | 28.26 |
| 5 | iPhone 5 | 22 | 1 | 40.23 |
| 6 | iPhone 5 | 22 | 5 | 38.81 |
| 7 | iPhone 5 | 22 | 10 | 37.87 |
| 8 | iPhone 5 | 22 | 5 | 39.81 |
| 9 | iPhone 5 | 22 | 1 | 40.13 |
| 10 | iPhone 5 | 22 | 10 | 42.85 |
| 11 | iPhone 5 | 22 | 10 | 43.05 |
| 12 | iPhone 5 | 22 | 10 | 36.00 |
| 13 | iPhone 5 | 22 | 5 | 41.80 |
| 14 | iPhone 5 | 22 | 5 | 39.73 |
| 15 | iPhone 5 | 40 | 5 | 22.79 |
| 16 | iPhone 5 | 30 | 1 | 26.48 |
| 17 | iPhone 5 | 40 | 1 | 23.53 |
| 18 | iPhone 5 | 40 | 10 | 20.60 |
| 20 | iPhone 5 | 22 | 5 | 41.35 |
| 21 | iPhone 5 | 22 | 10 | 58.77 |
| 22 | iPhone 5 | 30 | 10 | 15.73 |
| 23 | iPhone 5 | 22 | 10 | 9.38 |
| 24 | iPhone 5 | 30 | 10 | 27.36 |
| 25 | iPhone 5 | 30 | 10 | 32.34 |
| 27 | iPhone 5 | 22 | 5 | 40.81 |
| 28 | iPhone 5 | 30 | 1 | 31.71 |
| 29 | iPhone 5 | 22 | 10 | 40.79 |
| 30 | iPhone 5 | 22 | 1 | 39.93 |
| 31 | iPhone 5 | 22 | 1 | 18.74 |
| 32 | iPhone 5 | 22 | 1 | 39.82 |
| 33 | iPhone 5 | 30 | 5 | 28.43 |
| 34 | iPhone 5 | 22 | 5 | 38.66 |
| 35 | iPhone 5 | 22 | 1 | 42.51 |
| 36 | iPhone 5 | 22 | 1 | 41.83 |
| 37 | iPhone 5 | 22 | 10 | 44.14 |
| 38 | iPhone 5 | 30 | 5 | 31.09 |

| | | | | |
|---|---|---|---|---|
| 39 | iPhone 5c | 22 | 10 | 26.51 |
| 40 | iPhone 5c | 40 | 10 | 21.63 |
| 41 | iPhone 5c | 40 | 5 | 21.34 |
| 42 | iPhone 5c | 22 | 5 | 26.40 |
| 43 | iPhone 5c | 22 | 5 | 22.37 |
| 44 | iPhone 5c | 22 | 1 | 12.3 |
| 45 | iPhone 5c | 22 | 5 | 24.87 |
| 46 | iPhone 5c | 22 | 10 | 25.35 |
| 47 | iPhone 5c | 22 | 1 | 25.3 |
| 48 | iPhone 5c | 22 | 1 | 26.15 |
| 49 | iPhone 4 | 22 | 1 | 52.57 |
| 50 | iPhone 4 | 22 | 1 | 8.63 |
| 51 | iPhone 6 | 22 | 1 | 10.27 |
| 52 | iPhone 4 | 22 | 5 | 50.14 |
| 53 | iPhone 4 | 22 | 10 | 58.63 |
| 54 | iPhone 4 | 22 | 10 | 55.47 |
| 55 | iPhone 4 | 22 | 5 | 59.49 |
| 56 | iPhone 6 | 22 | 5 | 21.15 |
| 57 | iPhone 6 | 22 | 1 | 25.37 |
| 58 | iPhone 6 | 22 | 1 | 3.79 |
| 59 | iPhone 6plus | 22 | 1 | 27.76 |
| 19 | iPhone 5 | Failed | | |
| 26 | iPhone 5 | Failed | | |

# 11 Bibliography


Ambrosch, Roland, Ekaterina Ambrosch, Rainer Pamminger, Sebastian Glaser, and Max Regenfelder. 2018. “Automation of Smartphone Disassembly: Collabora-Tive Approach.” *International Conference on Going Green CARE INNOVATION*, 2–6.

Anderson, Eric H, Michael F Cash, Jonathan L Hall, and Gregory W Pettit. 2004. “Hexapods for Precision Motion and Vibration Control.” *Control of Precision Systems*, no. April: 1–5.

Bogue, Robert. 2019. “Robots in Recycling and Disassembly.” *Industrial Robot* 46 (4): 461–66. https://doi.org/10.1108/IR-03-2019-0053.

Borras, Julia, Raphael Heudorfer, Samuel Rader, Peter Kaiser, and Tamim Asfour. 2018. “The KIT Swiss Knife Gripper for Disassembly Tasks: A Multi-Functional Gripper for Bimanual Manipulation with a Single Arm.” *IEEE International Conference on Intelligent Robots and Systems*, 4590–97. https://doi.org/10.1109/IROS.2018.8593567.

Brogan, Daniel P., Nicholas M. DiFilippo, and Musa K. Jouaneh. 2021. “Deep Learning Computer Vision for Robotic Disassembly and Servicing Applications.” *Array* 12 (August): 100094. https://doi.org/10.1016/j.array.2021.100094.

Chen, Wei Hua, Kathrin Wegener, and Franz Dietrich. 2014. “A Robot Assistant for Unscrewing in Hybrid Human-Robot Disassembly.” *2014 IEEE International Conference on Robotics and Biomimetics, IEEE ROBIO 2014*, 536–41. https://doi.org/10.1109/ROBIO.2014.7090386.

Cui, Jirang, and Eric Forssberg. 2003. “Mechanical Recycling of Waste Electric and Electronic Equipment: A Review.” *Journal of Hazardous Materials* 99 (3): 243–63. https://doi.org/10.1016/S0304-3894(03)00061-X.

Diouf, Boucar, Ramchandra Pode, and Rita Osei. 2015. “Recycling Mobile Phone Batteries for Lighting.” *Renewable Energy* 78: 509–15. https://doi.org/10.1016/j.renene.2015.01.034.

Farag, Mohannad, Abdul Nasir Abd Ghafar, and Mohammed Hayyan Alsibai. 2019. “Grasping and Positioning Tasks for Selective Compliant Articulated Robotic Arm Using Object Detection and Localization: Preliminary Results.” *Proceedings - 2019 6th International Conference on Electrical and Electronics Engineering, ICEEE 2019*, 284–88. https://doi.org/10.1109/ICEEE2019.2019.00061.

Feng, Kai, Xianmin Zhang, Hai Li, and Yanjiang Huang. 2017. “A Dual-Camera Assisted Method of the

SCARA Robot for Online Assembly of Cellphone Batteries." *Lecture Notes in Computer Science (Including Subseries Lecture Notes in Artificial Intelligence and Lecture Notes in Bioinformatics)* 10463 LNAI: 576–87. https://doi.org/10.1007/978-3-319-65292-4_50.

Foo, Gwendolyn, Sami Kara, and Maurice Pagnucco. 2022a. "Artificial Learning for Part Identification in Robotic Disassembly Through Automatic Rule Generation in an Ontology." *IEEE Transactions on Automation Science and Engineering*, 1–14. https://doi.org/10.1109/TASE.2022.3149242.

Foo, Gwendolyn, Sami Kara, and Maurice Pagnucco. 2022b. "Challenges of Robotic Disassembly in Practice." *Procedia CIRP* 105: 513–18. https://doi.org/10.1016/j.procir.2022.02.085.

Ha, Vinh Hung, Jae chun Lee, Jinki Jeong, Huynh Trung Hai, and Manis K. Jha. 2010. "Thiosulfate Leaching of Gold from Waste Mobile Phones." *Journal of Hazardous Materials* 178 (1–3): 1115–19. https://doi.org/10.1016/j.jhazmat.2010.01.099.

He, Cheng, Zhongyan Jin, Runwei Gu, and Huaying Qu. 2020. "Automatic Disassembly and Recovery Device for Mobile Phone Circuit Board CPU Based on Machine Vision." *Journal of Physics: Conference Series* 1684 (1). https://doi.org/10.1088/1742-6596/1684/1/012137.

Kim, Yong Sik, Hongliang Shi, Nicholas Dagalakis, Jeremy Marvel, and Geraldine Cheok. 2019. "Design of a Six-DOF Motion Tracking System Based on a Stewart Platform and Ball-and-Socket Joints." *Mechanism and Machine Theory* 133: 84–94. https://doi.org/10.1016/j.mechmachtheory.2018.10.021.

Klas, Cornelius, Felix Hundhausen, Jianfeng Gao, Christian R.G. Dreher, Stefan Reither, You Zhou, and Tamim Asfour. 2021. "The KIT Gripper: A Multi-Functional Gripper for Disassembly Tasks." *Proceedings - IEEE International Conference on Robotics and Automation* 2021-May (Icra): 715–21. https://doi.org/10.1109/ICRA48506.2021.9561336.

Kopacek, P., and B. Kopacek. 2003. "Robotized Disassembly of Mobile Phones." *IFAC Proceedings Volumes* 36 (23): 103–5. https://doi.org/10.1016/s1474-6670(17)37669-3.

Lee, Jaeryeong, Youngjin Kim, and Jae chun Lee. 2012. "Disassembly and Physical Separation of Electric/Electronic Components Layered in Printed Circuit Boards (PCB)." *Journal of Hazardous Materials* 241–242: 387–94. https://doi.org/10.1016/j.jhazmat.2012.09.053.

Li, Hongrui, Huadong Sun, Fangshuo Fan, Hongguo Liu, Lin Li, and Fengfu Yin. 2022. "Research on an Intelligent Disassembling Method for Multi-Type Mobile Phones Based on Rough Set Theory."

*Procedia CIRP* 105: 547–52. https://doi.org/10.1016/j.procir.2022.02.091.

Li, Jia, Hongzhou Lu, Jie Guo, Zhenming Xu, and Yaohe Zhou. 2007. "Recycle Technology for Recovering Resources and Products from Waste Printed Circuit Boards." *Environmental Science and Technology* 41 (6): 1995–2000. https://doi.org/10.1021/es0618245.

Li, Jiawen, Xiaolong Song, Dong Yang, Bo Li, and Bin Lu. 2019. "Simulating the Interprovincial Movements of Waste Mobile Phones in China Based on the Current Disassembly Capacity." *Journal of Cleaner Production* 244. https://doi.org/10.1016/j.jclepro.2019.118776.

Lisińska, M., M. Saternus, and J. Willner. 2018. "Research of Leaching of the Printed Circuit Boards Coming from Waste Mobile Phones." *Archives of Metallurgy and Materials* 63 (1): 143–47. https://doi.org/10.24425/118921.

Liu, Hongguo, Jingjing Hai, Lin Li, and Fengfu Yin. 2022. "An Efficient Disassembly Process Generation Method for Large Quantities of Waste Smartphones." *Procedia CIRP* 105: 140–45. https://doi.org/10.1016/j.procir.2022.02.024.

M. H. Khamsehei Fadaei, S. A. Hamzeh Pahnehkolaei, M. J. Hesarlou and Z. Torkan. 2017. "Dynamics Modeling of a Stewart Platform in Simulink MSC ADAMS." *2017 IEEE 4th International Conference on Knowledge-Based Engineering and Innovation (KBEI)*, 294–98. https://doi.org/10.1109/KBEI.2017.8324989.

Ma, Nan, Xin Dong, David Palmer, Josue Camacho Arreguin, Zhirong Liao, Mingfeng Wang, and Dragos Axinte. 2019. "Parametric Vibration Analysis and Validation for a Novel Portable Hexapod Machine Tool Attached to Surfaces with Unequal Stiffness." *Journal of Manufacturing Processes* 47 (January): 192–201. https://doi.org/10.1016/j.jmapro.2019.10.003.

Mangold, Simon, Christian Steiner, Marco Friedmann, and Jürgen Fleischer. 2022. "Vision-Based Screw Head Detection for Automated Disassembly for Remanufacturing." *Procedia CIRP* 105: 1–6. https://doi.org/10.1016/j.procir.2022.02.001.

McCann, Connor M., and Aaron M. Dollar. 2018. "Analysis and Dimensional Synthesis of a Robotic Hand Based on the Stewart-Gough Platform." *Proceedings of the ASME Design Engineering Technical Conference* 5A-2018: 1–8. https://doi.org/10.1115/DETC201886149.

Mehmet I. Sarigecili*, Mehmet Murat Baysal, Bicheng Zhu and Utpal Roy Department. 2013. "A Disassembly Process Model for End-of-Life Activities of Manufactured Products Mehmet I .

Sarigecili *, Mehmet Murat Baysal , Bicheng Zhu and Utpal Roy" 3 (1): 37–56.

Murthy, Venkatesha, and Seeram Ramakrishna. 2022. "A Review on Global E-Waste Management: Urban Mining towards a Sustainable Future and Circular Economy." *Sustainability (Switzerland)* 14 (2). https://doi.org/10.3390/su14020647.

Osibanjo, Oladele, and Innocent Chidi Nnorom. 2008. "Material Flows of Mobile Phones and Accessories in Nigeria: Environmental Implications and Sound End-of-Life Management Options." *Environmental Impact Assessment Review* 28 (2–3): 198–213. https://doi.org/10.1016/j.eiar.2007.06.002.

Patel, Y. D., and P. M. George. 2012. "Parallel Manipulators Applications—A Survey." *Modern Mechanical Engineering* 02 (03): 57–64. https://doi.org/10.4236/mme.2012.23008.

Rujanavech, Charissa, Joe Lessard, Chandler Sarah, Shannon Sean, Dahmus Jeffrey, and Guzzo Rob. 2016. "Liam - An Innovation Story." *Electronics Goes Green 2016+*, no. September: 1–4.

Sanito, Raynard Christianson, Sheng Jie You, and Ya Fen Wang. 2021. "Application of Plasma Technology for Treating E-Waste: A Review." *Journal of Environmental Management* 288 (200): 112380. https://doi.org/10.1016/j.jenvman.2021.112380.

Schumacher, Paul, and Musa Jouaneh. 2013. "A System for Automated Disassembly of Snap-Fit Covers." *International Journal of Advanced Manufacturing Technology* 69 (9–12): 2055–69. https://doi.org/10.1007/s00170-013-5174-8.

Shittu, O. S., I. D. Williams, and P. J. Shaw. 2021. "The 'WEEE' Challenge: Is Reuse the 'New Recycling'?" *Resources, Conservation and Recycling* 174 (July): 105817. https://doi.org/10.1016/j.resconrec.2021.105817.

Short, Elaine Schaertl, Dale Short, Yifeng Fu, and Maja J. Matarić. 2017. "SPRITE: Stewart Platform Robot for Interactive Tabletop Engagement." *University of Southern California, Department of Computer Science Technical Report*, 17–970. https://www.cs.usc.edu/sites/default/files/field/file/17-970 SPRITE-Stewart Platform Robot for Interactive Tabletop Engagement.pdf.

Tang, Jie, Dengqing Cao, and Tianhu Yu. 2019. "Decentralized Vibration Control of a Voice Coil Motor-Based Stewart Parallel Mechanism: Simulation and Experiments." *Proceedings of the Institution of Mechanical Engineers, Part C: Journal of Mechanical Engineering Science* 233 (1): 132–45. https://doi.org/10.1177/0954406218756941.

Virgil Petrescu, Relly Victoria, Raffaella Aversa, Antonio Apicella, Samuel Kozaitis, Taher Abu-Lebdeh, and Florian Ion Tiberiu Petrescu. 2018. “Inverse Kinematics of a Stewart Platform.” *Journal of Mechatronics and Robotics* 2 (1): 45–59. https://doi.org/10.3844/jmrsp.2018.45.59.

Wang, Zeli, Heng Li, and Xiaoling Zhang. 2019. “Construction Waste Recycling Robot for Nails and Screws: Computer Vision Technology and Neural Network Approach.” *Automation in Construction* 97 (November 2018): 220–28. https://doi.org/10.1016/j.autcon.2018.11.009.

Wapler, Matthias, Volker Urban, Thomas Weisener, Jan Stallkamp, Mark Dürr, and Andrea Hiller. 2003. “A Stewart Platform for Precision Surgery.” *Transactions of the Institute of Measurement & Control* 25 (4): 329–34. https://doi.org/10.1191/0142331203tm092oa.

Windisch-Kern, Stefan, Eva Gerold, Thomas Nigl, Aleksander Jandric, Michael Altendorfer, Bettina Rutrecht, Silvia Scherhaufer, et al. 2022. “Recycling Chains for Lithium-Ion Batteries: A Critical Examination of Current Challenges, Opportunities and Process Dependencies.” *Waste Management* 138: 125–39. https://doi.org/10.1016/j.wasman.2021.11.038.

Yang, Chao, Wei Ye, and Qinchuan Li. 2022. “Review of the Performance Optimization of Parallel Manipulators.” *Mechanism and Machine Theory* 170 (January): 104725. https://doi.org/10.1016/j.mechmachtheory.2022.104725.

Yildiz, Erenus, Tobias Brinker, Erwan Renaudo, Jakob J. Hollenstein, Simon Haller-Seeber, Justus Piater, and Florentin Wörgötter. 2020. “A Visual Intelligence Scheme for Hard Drive Disassembly in Automated Recycling Routines.” *ROBOVIS 2020 - Proceedings of the International Conference on Robotics, Computer Vision and Intelligent Systems*, no. November: 17–27. https://doi.org/10.5220/0010016000170027.

Yildiz, Erenus, and Florentin Wörgötter. 2020. “DCNN-Based Screw Classification in Automated Disassembly Processes.” *ROBOVIS 2020 - Proceedings of the International Conference on Robotics, Computer Vision and Intelligent Systems*, no. November: 61–68. https://doi.org/10.5220/0009979900610068.

Zhang, Guoliang, Songmin Jia, Dishi Zeng, and Zeling Zheng. 2019. “Object Detection and Grabbing Based on Machine Vision for Service Robot.” *2018 IEEE 9th Annual Information Technology, Electronics and Mobile Communication Conference, IEMCON 2018*, 89–94. https://doi.org/10.1109/IEMCON.2018.8615062.